Characterizing the Mean-field Dynamo
in weakly magnetized turbulent accretion disks

Oliver Gressel ⋆
Niels Bohr International Academy, Copenhagen

Martín Pessah (NBIA, Copenhagen)
Axel Brandenburg (Nordita, Stockholm)
Udo Ziegler (AIP, Potsdam)

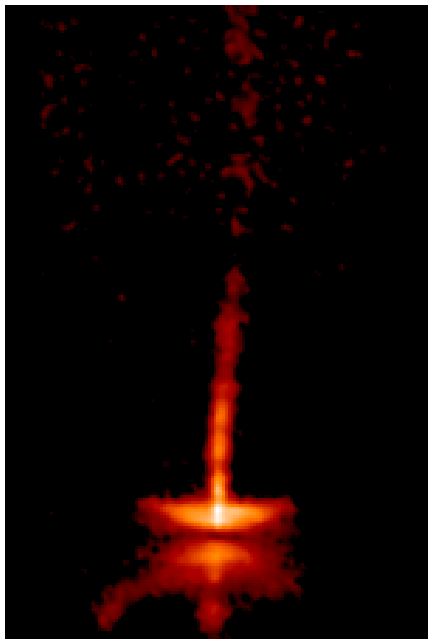

February 2nd, 2017

⋆ gressel@nbi.ku.dk

talk outline

talk outline

1. Accretion disk dynamos
   - The need for a dynamo mechanism
   - Mean-field MHD in a nutshell
   - Constraints from helicity conservation

2. Challenges and new aspects
   - Finite thermal conductivity
   - Parameter studies as a fruitful test-bed?
   - Non-locality of mean-field effects

the engine: magnetorotational instability

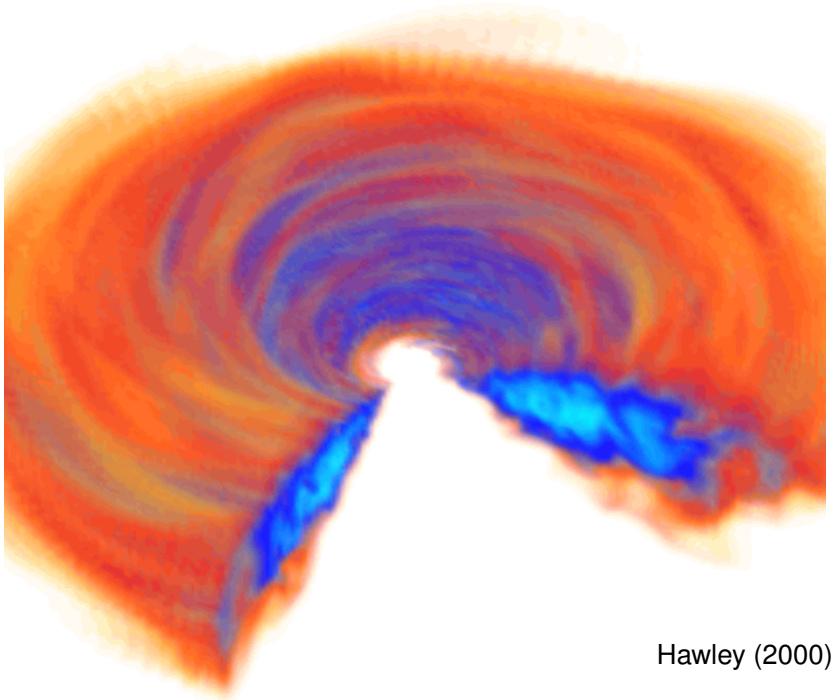

Hawley (2000)

- accretion luminosity via turbulent viscosity
- weak magnetic fields destabilise shear flow
  MRI, Balbus & Hawley (1991)
- robust linear instability – problem solved ...

- ... twenty-five years later, saturation mechanism remains enigmatic
- attempts
  - ? linear theory
  - ? direct simulations
  - ? parasitic instabilities
  - ? mean-field dynamo

the key: survival of large-scale coherent fields

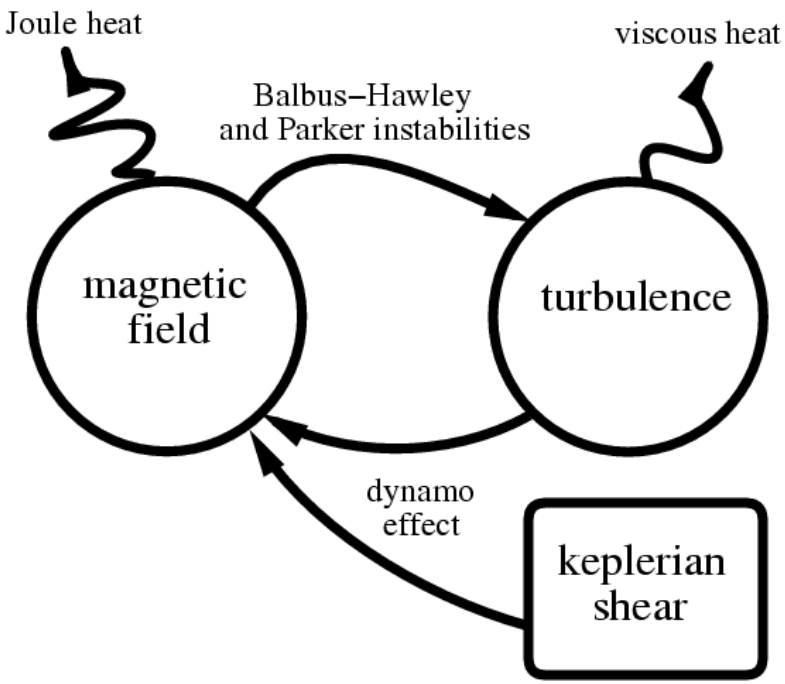

Brandenburg (1995)

- stratified shearing boxes have all ingredients for a classical strato-cyclonic dynamo
- large-scale dynamo is less likely Pm-dependent Brandenb (2001)
- tall-enough (un-)stratified ZNF converged (?!) Davis, Stone & Pessah (2010), Shi, Stone & Huang (2016)
- (cyclic) dynamo already seen in unstratified ZNF case Lesur & Ogilvie (2008), Herault et al. (2013/15) Squire & Bhattacharjee (2015a/b)

- complementary route: study evolution of embedded poloidal flux

the key: survival of large-scale coherent fields

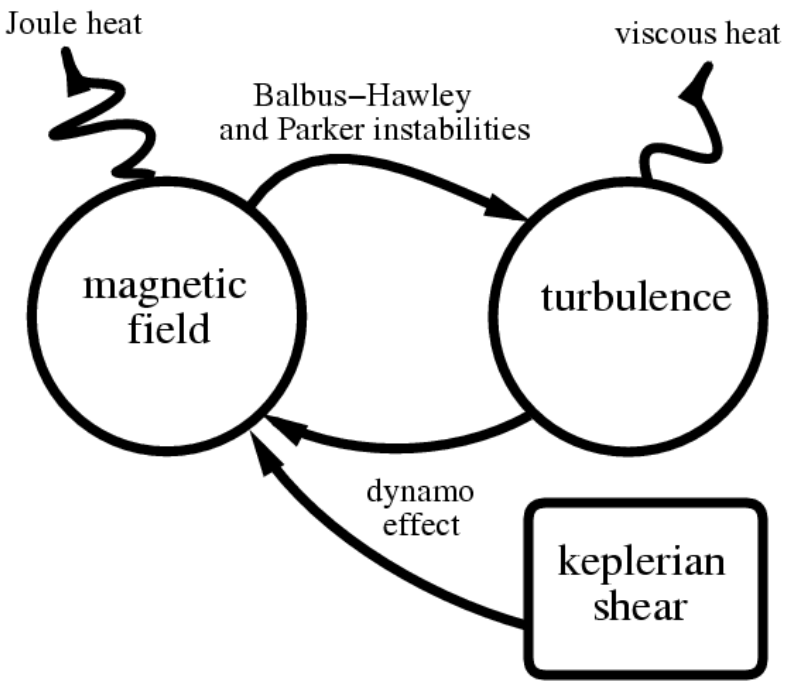

Brandenburg (1995)

- stratified shearing boxes have all ingredients for a classical strato-cyclonic dynamo
- large-scale dynamo is less likely Pm-dependent Brandenb (2001)
- tall-enough (un-)stratified ZNF converged (?!) Davis, Stone & Pessah (2010), Shi, Stone & Huang (2016)
- (cyclic) dynamo already seen in unstratified ZNF case Lesur & Ogilvie (2008), Herault et al. (2013/15) Squire & Bhattacharjee (2015a/b)

- complementary route: study evolution of embedded poloidal flux

MRI dynamo versus MHD dynamo

$$\mathbf{u}^{\rm ch} = u_0\, F\!\left(\tfrac{z}{H}\right) \mathrm{e}^{st}\, [\mathbf{e}_x\, \cos\theta + \mathbf{e}_y\, \sin\theta]$$
$$\mathbf{B}^{\rm ch} = B_0\, G\!\left(\tfrac{z}{H}\right) \mathrm{e}^{st}\, [\mathbf{e}_x\, \sin\theta - \mathbf{e}_y\, \cos\theta]$$

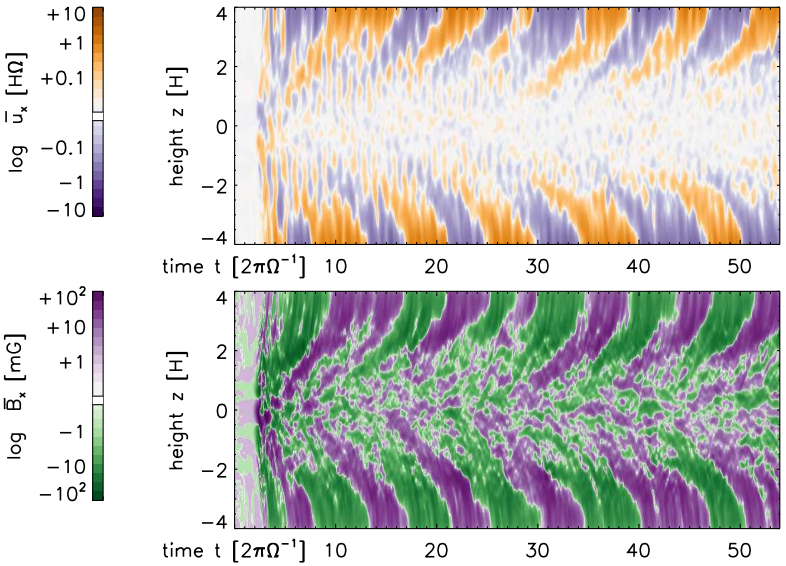

model 'A1' from Gressel, Nelson & Turner (2011)

dynamo effect due to EMF from
MC waves / MRI modes / parasites ?!

see e.g. Ebrahimi, Prager & Schnack (2009), Riols et al. (2016)

strong fields → low wave-number

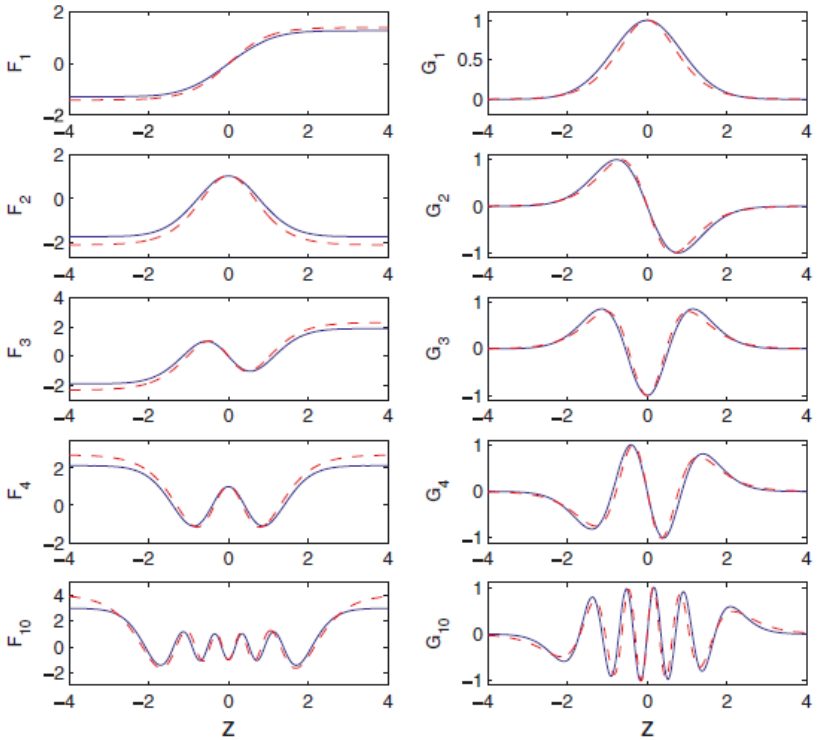

Latter, Fromang & Gressel (2010)

weak fields → high wave-number

the mean induction equation

$$\partial_t \overline{\bar{\mathbf{B}} + \mathbf{B}'} = \nabla \times \overline{\left[(\bar{\mathbf{u}} + \mathbf{u}') \times (\bar{\mathbf{B}} + \mathbf{B}') \right]} + \eta \nabla^2 \overline{\bar{\mathbf{B}} + \mathbf{B}'}$$

- Reynold's averaging rules:
  - idempotence: $\bar{\bar{f}} = \bar{f}$
  - symmetric perturbations: $\overline{f'} = 0$
  - summation: $\overline{f + g} = \bar{f} + \bar{g}$
  - mixed product: $\overline{\bar{f} \times g'} = \bar{\bar{f}} \times \bar{g'} = 0$
- mean-field induction equation

$$\partial_t \bar{\mathbf{B}} = \nabla \times (\bar{\mathbf{u}} \times \bar{\mathbf{B}}) + \nabla \times \bar{\mathcal{E}} + \eta \nabla^2 \bar{\mathbf{B}}$$

with turbulent EMF $\bar{\mathcal{E}} = \overline{\mathbf{u}' \times \mathbf{B}'}$ subsuming small-scale effects

a closure relation for large-scale coherent fields

- mean-field induction equation:

$$\partial_t \bar{\mathbf{B}} = \nabla \times (\bar{\mathbf{u}} \times \bar{\mathbf{B}}) + \nabla \times \bar{\mathcal{E}} + \eta \nabla^2 \bar{\mathbf{B}}$$

with turbulent EMF $\bar{\mathcal{E}} = \overline{\mathbf{u}' \times \mathbf{B}'}$ subsuming small-scale effects

- aim: find an evolution equation for the mean EMF

$$\bar{\mathcal{E}}(z,t) = \overline{\mathbf{u}'(z,t) \times \mathbf{B}'(z,t)} = \overline{\mathbf{u}'(z,t) \times \int_{\tau=0}^{t} \partial_\tau \mathbf{B}'(z,\tau)\, \mathrm{d}\tau} \; + \; \ldots$$

- compute magnetic field fluctuations:

$$\begin{aligned}
\partial_t(\bar{\mathbf{B}} + \mathbf{B}') &= \nabla \times \left[(\bar{\mathbf{u}} + \mathbf{u}') \times (\bar{\mathbf{B}} + \mathbf{B}')\right] + \eta \nabla^2 (\bar{\mathbf{B}} + \mathbf{B}') \\
\ominus \quad \partial_t \bar{\mathbf{B}} &= \nabla \times [\bar{\mathbf{u}} \times \bar{\mathbf{B}} + \overline{\mathbf{u}' \times \mathbf{B}'}] + \eta \nabla^2 \bar{\mathbf{B}} \\
\hline
\partial_t \mathbf{B}' &= \nabla \times [\, \bar{\mathbf{u}} \times \mathbf{B}' + \mathbf{u}' \times \mathbf{B}' - \overline{\mathbf{u}' \times \mathbf{B}'} + \mathbf{u}' \times \bar{\mathbf{B}} - \eta \nabla \times \mathbf{B}' \,]
\end{aligned}$$

- third-order moments appear when substituted into $\bar{\mathcal{E}}(z,t)$
- ad-hoc parametrisation $\bar{\mathcal{E}}_i = \alpha_{ij} \bar{B}_j - \tilde{\eta}_{ij}\, \varepsilon_{jkl} \partial_k \bar{B}_l$

closure ansatz for MF-MHD

- parametrise turbulent EMF as a functional of $\bar{\mathbf{u}}$, $\bar{\mathbf{B}}$, $\overline{f(\mathbf{u}')}$
  - $$\bar{\mathcal{E}}_i = \alpha_{ij}\bar{B}_j + \eta_{ijk}\partial_k\bar{B}_j \quad = \alpha_{ij}\bar{B}_j - \tilde{\eta}_{ij}\,\varepsilon_{jkl}\partial_k\bar{B}_l$$
- Interpretation of parameters for $\bar{\mathbf{B}} = \bar{\mathbf{B}}(z)$:

$$\bar{\mathcal{E}} = \begin{pmatrix} \alpha_R & -\gamma_z & 0 \\ \gamma_z & \alpha_\phi & 0 \\ 0 & 0 & \alpha_z \end{pmatrix} \bar{\mathbf{B}} - \begin{pmatrix} \tilde{\eta}_R & \delta_z & 0 \\ -\delta_z & \tilde{\eta}_\phi & 0 \\ 0 & 0 & \tilde{\eta}_z \end{pmatrix} \nabla\times\bar{\mathbf{B}}$$

  - diagonal elements of α give dynamo-effect
  - vertical turbulent pumping is contained in γ_z
  - diagonals of $\tilde{\eta}$ give turbulent diffusivity
  - off-diagonals $\rightarrow \Omega \times J$ effect, Rädler (1969)

the test-field approach

- Determine dynamo parameters from DNS:
  - inversion of tensor equation
  - non-trivial for $B_x \simeq B_y$

$$\bar{\mathcal{E}}_i = \alpha_{ij}\bar{B}_j + \eta_{ijk}\partial_k\bar{B}_j$$

- Test-field method (Schrinner et al., 2005, 2007):
  - invert above equation for well behaved test-fields
  - defined gradient of test-field allows to solve for diffusivity
  - comes at the price of solving a passive induction equation for the fluctuations belonging to each (constant) test-field $\bar{\mathcal{B}}_{(\nu)}$:

$$\begin{aligned}\partial_t \mathcal{B}'_{(\nu)} = \quad \nabla\times \quad & [\,\bar{\mathbf{u}}\times\mathcal{B}'_{(\nu)} + \mathbf{u}'\times\mathcal{B}'_{(\nu)} \\ & -\overline{\mathbf{u}'\times\mathcal{B}'_{(\nu)}} + \mathbf{u}'\times\bar{\mathcal{B}}_{(\nu)} - \eta\nabla\times\mathcal{B}'_{(\nu)}\,]\end{aligned}$$

  - underlying DNS can be HD (kinematic case)
  - quenching will depend on actual field for MHD-runs

the test-field approach

- Determine dynamo parameters from DNS:
  - inversion of tensor equation
  - non-trivial for $B_x \simeq B_y$

$$\bar{\mathcal{E}}_i = \alpha_{ij}\bar{B}_j + \eta_{ijk}\partial_k\bar{B}_j$$

- Test-field method (Schrinner et al., 2005, 2007):
  - invert above equation for well behaved test-fields
  - defined gradient of test-field allows to solve for diffusivity
  - comes at the price of solving a passive induction equation for the fluctuations belonging to each (constant) test-field $\bar{\mathcal{B}}_{(\nu)}$:

$$\begin{aligned}\partial_t\mathcal{B}'_{(\nu)} = \quad \nabla\times \quad & [\,\bar{\mathbf{u}}\times\mathcal{B}'_{(\nu)} + \mathbf{u}'\times\mathcal{B}'_{(\nu)} \\ & -\overline{\mathbf{u}'\times\mathcal{B}'_{(\nu)}} + \mathbf{u}'\times\bar{\mathcal{B}}_{(\nu)} - \eta\nabla\times\mathcal{B}'_{(\nu)}\,]\end{aligned}$$

  - underlying DNS can be HD (kinematic case)
  - quenching will depend on actual field for MHD-runs

harmonic test fields as diagnostic

- Choice of test-fields:
  - wave number $k_1 \equiv \pi/L_z$, new: k-dependent
  - harmonic test-field perturbations Brandenburg (2005)

$$\bar{\mathcal{B}}_{(0)} = \cos(k_1 z)\,\hat{\mathbf{x}}\,, \qquad \bar{\mathcal{B}}_{(1)} = \sin(k_1 z)\,\hat{\mathbf{x}}\,,$$
$$\bar{\mathcal{B}}_{(2)} = \cos(k_1 z)\,\hat{\mathbf{y}}\,, \qquad \bar{\mathcal{B}}_{(3)} = \sin(k_1 z)\,\hat{\mathbf{y}}\,.$$

  - solve $\bar{\mathcal{E}}_i = \alpha_{ij}\bar{\mathcal{B}}_j - \eta_{ijk}\partial_k\bar{\mathcal{B}}_j$ via

$$\begin{pmatrix} \alpha_{ij} \\ k_1\eta_{ij3} \end{pmatrix} = \begin{pmatrix} \cos(k_1 z) & \sin(k_1 z) \\ -\sin(k_1 z) & \cos(k_1 z) \end{pmatrix} \begin{pmatrix} \bar{\mathcal{E}}_i^{(2j-2)} \\ \bar{\mathcal{E}}_i^{(2j-1)} \end{pmatrix}$$

    - with $\bar{\mathcal{E}}^{(\nu)}(z,t) = \overline{\mathbf{u}' \times \mathcal{B}'_{(\nu)}}$ computed from the evolved TF fluctuations $\mathcal{B}'_{(\nu)}(x,y,z,t)$, and with $\mathbf{u}'(x,y,z,t)$ from DNS
    - "quasi"-kinematic $\rightarrow$ formally valid for MRI (but concerns remain about dynamically relevant background turbulence / small-scale dynamo)

harmonic test fields as diagnostic

- Choice of test-fields:
  - wave number $k_1 \equiv \pi/L_z$, new: k-dependent
  - harmonic test-field perturbations Brandenburg (2005)

$$\bar{\mathcal{B}}_{(0)} = \cos(k_1 z)\,\hat{\mathbf{x}}\,, \qquad \bar{\mathcal{B}}_{(1)} = \sin(k_1 z)\,\hat{\mathbf{x}}\,,$$
$$\bar{\mathcal{B}}_{(2)} = \cos(k_1 z)\,\hat{\mathbf{y}}\,, \qquad \bar{\mathcal{B}}_{(3)} = \sin(k_1 z)\,\hat{\mathbf{y}}\,.$$

  - solve $\bar{\mathcal{E}}_i = \alpha_{ij}\bar{\mathcal{B}}_j - \eta_{ijk}\partial_k\bar{\mathcal{B}}_j$ via

$$\begin{pmatrix} \alpha_{ij} \\ k_1\eta_{ij3} \end{pmatrix} = \begin{pmatrix} \cos(k_1 z) & \sin(k_1 z) \\ -\sin(k_1 z) & \cos(k_1 z) \end{pmatrix} \begin{pmatrix} \bar{\mathcal{E}}_i^{(2j-2)} \\ \bar{\mathcal{E}}_i^{(2j-1)} \end{pmatrix}$$

    - with $\bar{\mathcal{E}}^{(\nu)}(z,t) = \overline{\mathbf{u}' \times \mathcal{B}'_{(\nu)}}$ computed from the evolved TF fluctuations $\mathcal{B}'_{(\nu)}(x,y,z,t)$, and with $\mathbf{u}'(x,y,z,t)$ from DNS
    - "quasi"-kinematic $\rightarrow$ formally valid for MRI (but concerns remain about dynamically relevant background turbulence / small-scale dynamo)

derived dynamo models

- idea: build simple model based on diagnostics
- works splendidly well for interstellar turbulence . . .

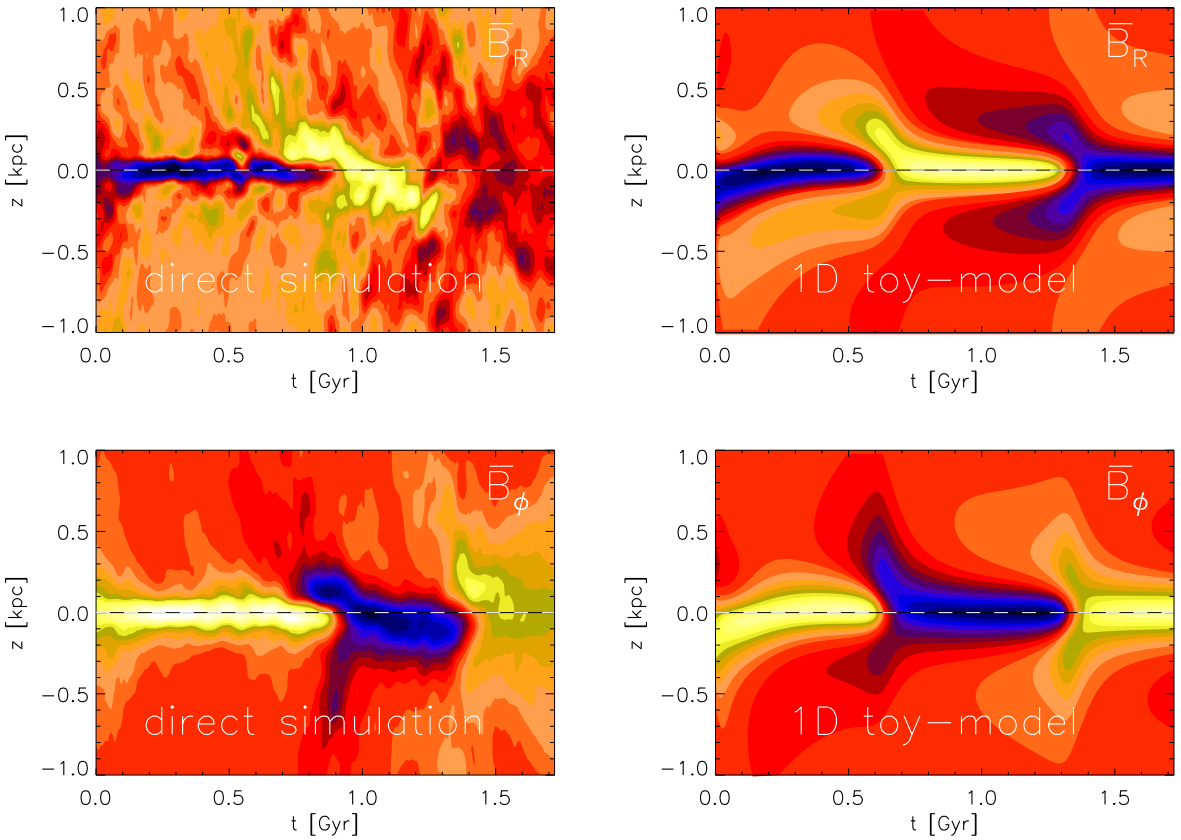

beyond the kinematic phase

- Dynamical quenching (new notation: $a = A'$, $b = B'$, ...)
  - non-linear effects in the EMF

$$\partial_t \bar{\mathcal{E}} = \overline{u \times (\partial_t b)} + \overline{(\partial_t u) \times b}$$

$$\rightarrow \qquad \alpha = \alpha_{\mathrm{K}} + \alpha_{\mathrm{M}} = -\tfrac{1}{3}\tau_{\mathrm{K}} \langle \omega \cdot u \rangle + \tfrac{1}{3}\tau_{\mathrm{M}} \langle j \cdot b \rangle / \rho$$

  - magnetic helicity evolution

$$\partial_t \langle \bar{A} \cdot \bar{B} \rangle = +2 \langle \bar{\mathcal{E}} \cdot \bar{B} \rangle - 2\eta \langle \bar{J} \cdot \bar{B} \rangle$$

$$\partial_t \langle a \cdot b \rangle = -2 \langle \bar{\mathcal{E}} \cdot \bar{B} \rangle - 2\eta \langle j \cdot b \rangle$$

  - time evolution for effective α effect

$$\partial_t \alpha = -2\eta_{\mathrm{t}} k_{\mathrm{f}}^2 \left(\frac{\alpha \langle \bar{B}^2 \rangle - \eta_{\mathrm{t}} \langle \bar{J} \cdot \bar{B} \rangle + \text{fluxes}}{B_{\mathrm{eq}}^2} + \frac{\alpha - \alpha_{\mathrm{K}}}{\eta_t / \eta} \right)$$

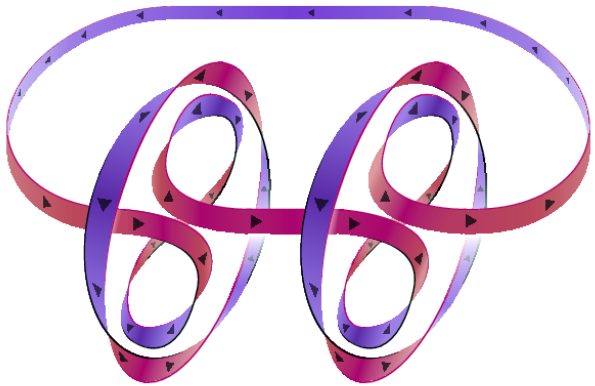

Blackman (2014)

using $\alpha_{\mathrm{K}} = \text{const.}$, $\langle \bar{\mathcal{E}} \cdot \bar{B} \rangle = \langle \alpha \bar{B} \cdot \bar{B} \rangle - \langle \eta_{\mathrm{t}} \bar{J} \cdot \bar{B} \rangle$ and $\langle a \cdot b \rangle \simeq k_{\mathrm{f}}^{-2} \langle j \cdot b \rangle$

- Blackman & Field (2000)
- Vishniac & Cho (2001)
- Blackman & Brandenburg (2002)
- Vishniac & Shapovalov (2014)
- Squire & Bhattacharjee (2015a/b)

quenching scenarios

- Stationary-state, dynamical quenching
  - general form ($\mathrm{d}\alpha/\mathrm{d}t = 0$):

$$\alpha = \frac{\alpha_{\rm K} + \eta_{\rm t}{\rm Rm}\langle\bar{J}\cdot\bar{B}/B_{\rm eq}^2\rangle + \text{fluxes}}{1 + {\rm Rm}\,\langle\bar{B}^2\rangle/B_{\rm eq}^2}$$

  - catastrophic quenching ($\bar{J} = 0$, no fluxes):

$$\alpha = \frac{\alpha_{\rm K}}{1 + {\rm Rm}\,\langle\bar{B}^2\rangle/B_{\rm eq}^2}$$

  - fully helical large-scale field ($\langle\,\bar{J}\cdot\bar{B}\,\rangle = k_{\rm m}\bar{B}^2$):

$$\alpha = \frac{\alpha_{\rm K} + \eta_{\rm t}\,k_{\rm m}\,{\rm Rm}\langle\bar{B}^2\rangle/B_{\rm eq}^2}{1 + {\rm Rm}\,\langle\bar{B}^2\rangle/B_{\rm eq}^2} \to k_{\rm m}\,\eta_{\rm t}$$

    Compared to the kinematic value $\alpha_{\rm K} \simeq k_{\rm f}\,\eta_{\rm t}$,
    α is quenched by the scale-separation ratio $k_{\rm m}/k_{\rm f}$.

interstellar turbulence

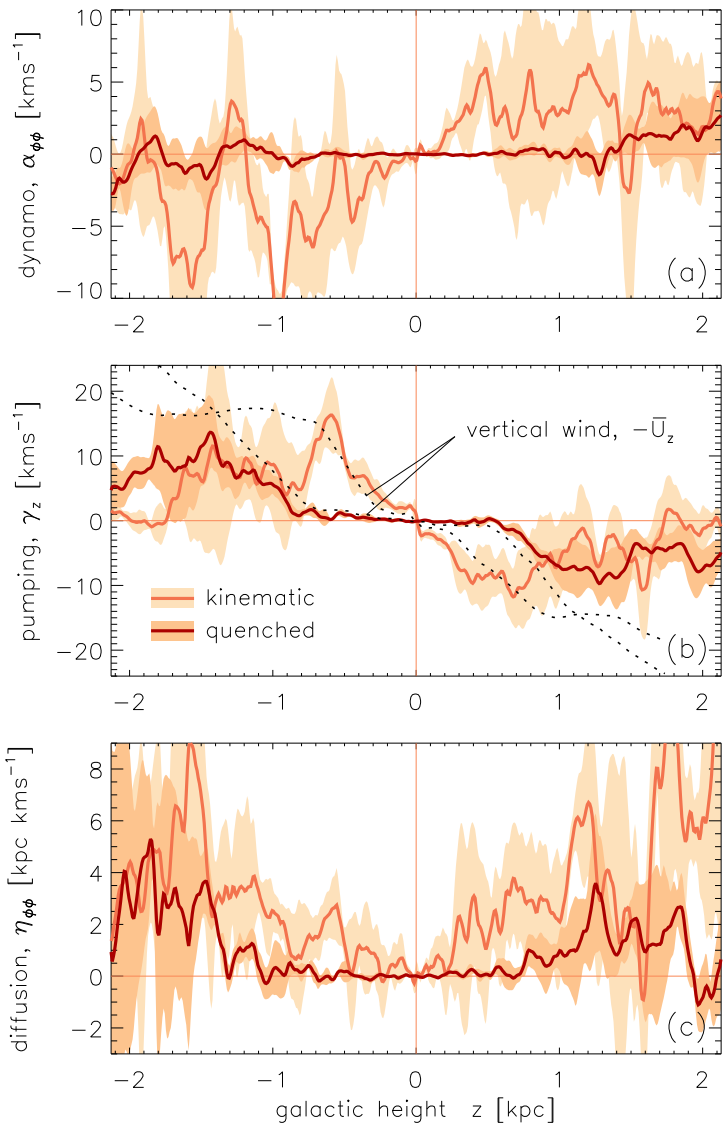

- Quenching scenarios:
  - (a) classic: flow quenching due to Lorentz force
  - (b) catastrophic: helicity conservation inhibits growth
  - (c) similar to scenario (b) but alleviated by small-scale helicity removal
- Test possible realisations:
  - quenching sets-in . . .
    (a) . . . at $B \simeq B_{\rm eq}$
    (b) . . . at $B \simeq B_{\rm eq}/{\rm Rm}$
    (c) . . . at $B \simeq B_{\rm eq}\, l_0/L_0$

Gressel, Bendre & Elstner (2013), MNRAS 429, 967

extracting quenching functions

- quenching quadratic in $\beta \equiv \bar{B}/B_{\rm eq}$
- magnetic Reynolds number, $\mathrm{Rm} \equiv u_{\rm rms}(k_{\rm f}\,\eta)^{-1} \simeq 75$–$125$
- scale separation ratio, $l_0/L_0 \simeq 0.1\,\mathrm{kpc}/1\,\mathrm{kpc} = 10$

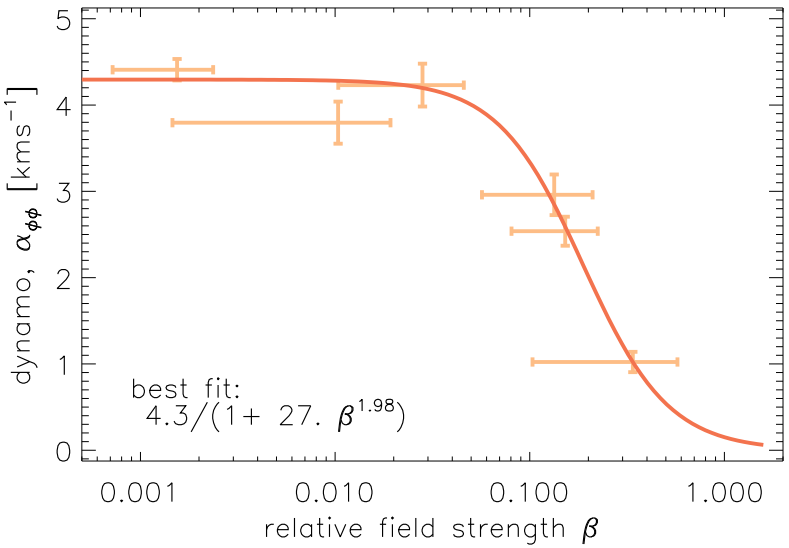

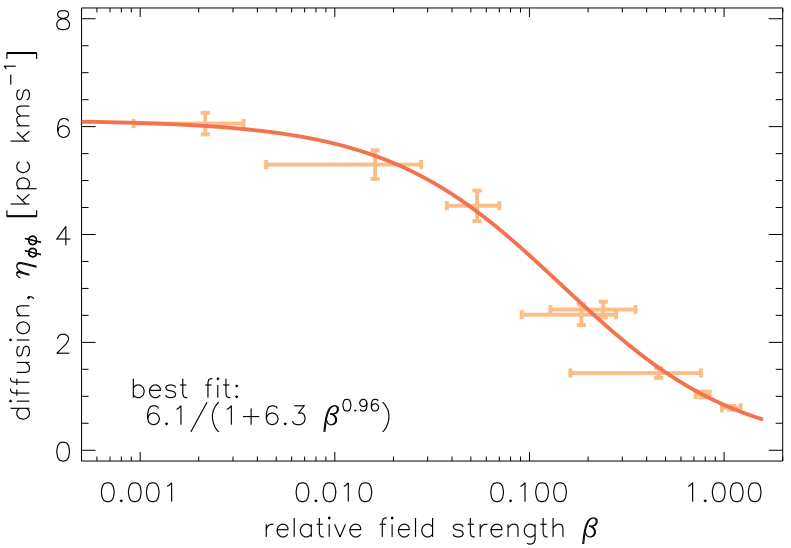

Gressel, Bendre & Elstner (2013), MNRAS 429, 967

dynamically quenched mean-field model

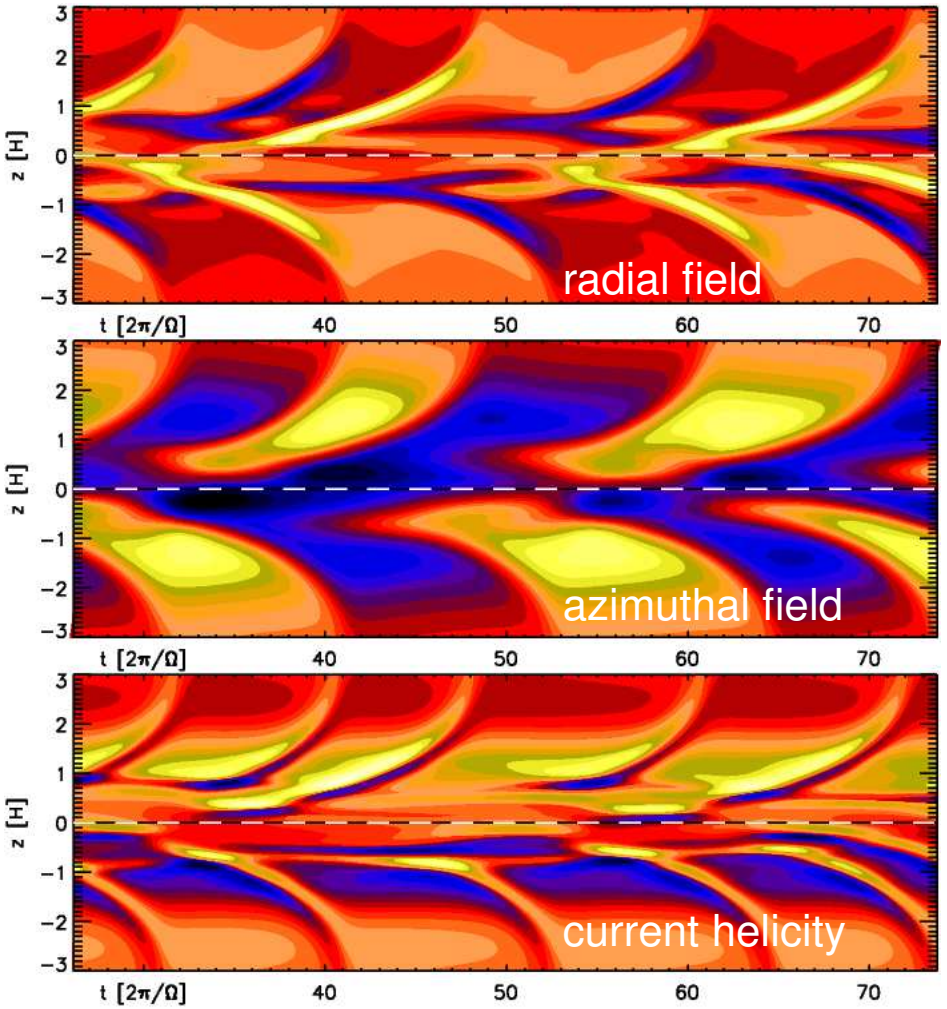

Gressel (2010), MNRAS 405, 41

- reproduces decently qualitative features:
  - asymmetry in B_R and B_ϕ
  - intermittent parity, chaotic features (Rm dependent)
  - frequency doubling in helicity (phase shift)
- quantitative agreement difficult due to sensitive parameter dependencies

dynamically quenched mean-field model

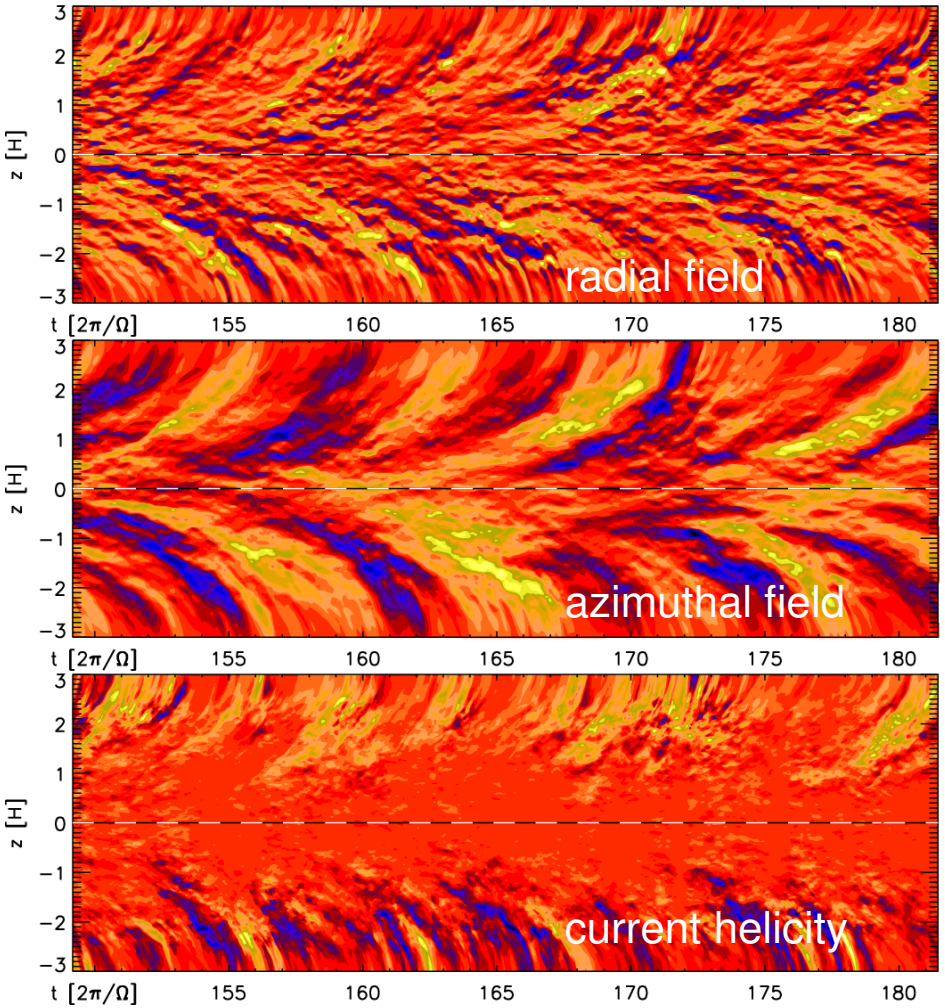

Gressel (2010), MNRAS 405, 41

- reproduces decently qualitative features:
  - asymmetry in B_R and B_ϕ
  - intermittent parity, chaotic features (Rm dependent)
  - frequency doubling in helicity (phase shift)
- quantitative agreement difficult due to sensitive parameter dependencies

non-isothermal simulations

- effects of turbulent convection vs. thermal conduction
- dynamo boosted by overturning convection Bodo et al. (2013a/b), Hirose (2014)
- butterfly “locked” during convective epoch Coleman et al. (2017)

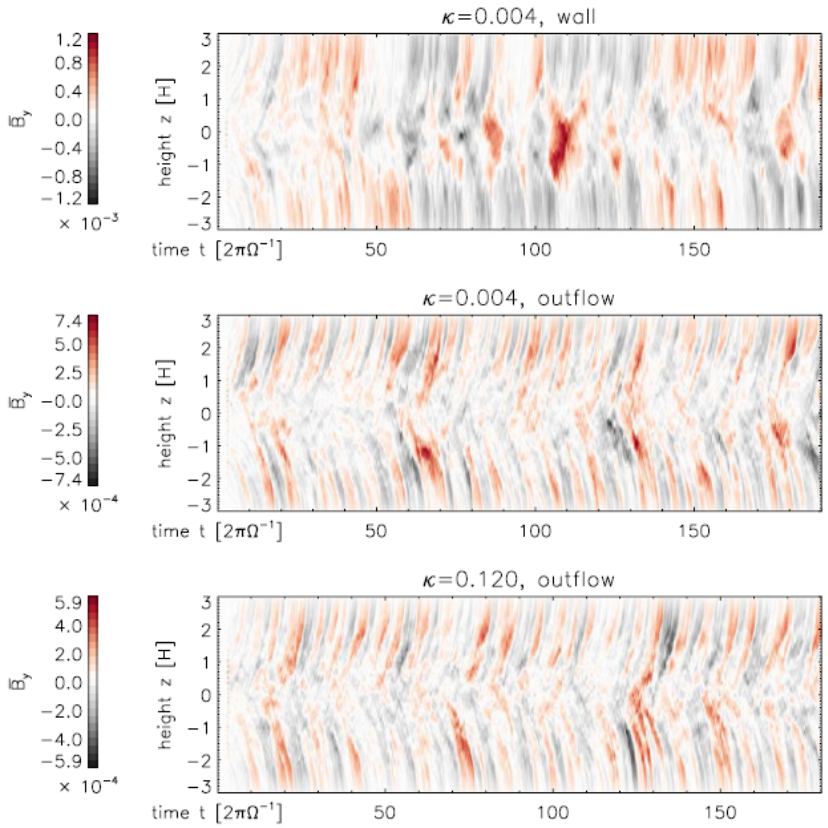

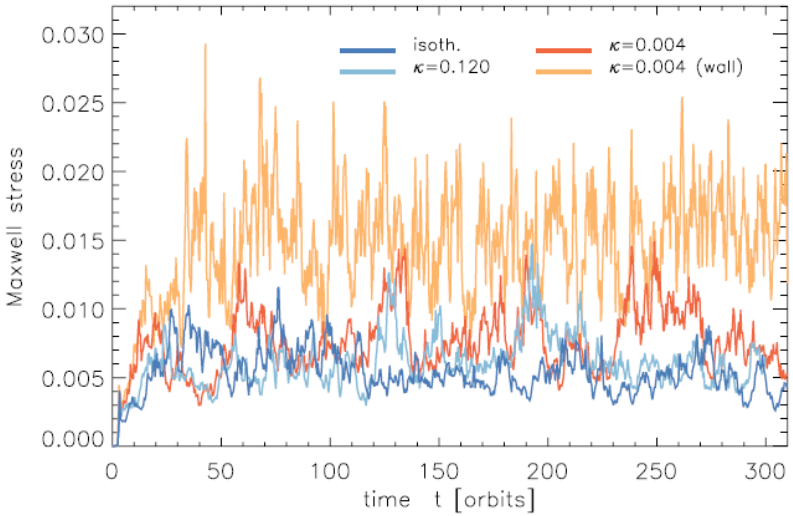

Gressel (2013), ApJ 770, 100

vertical disc structure

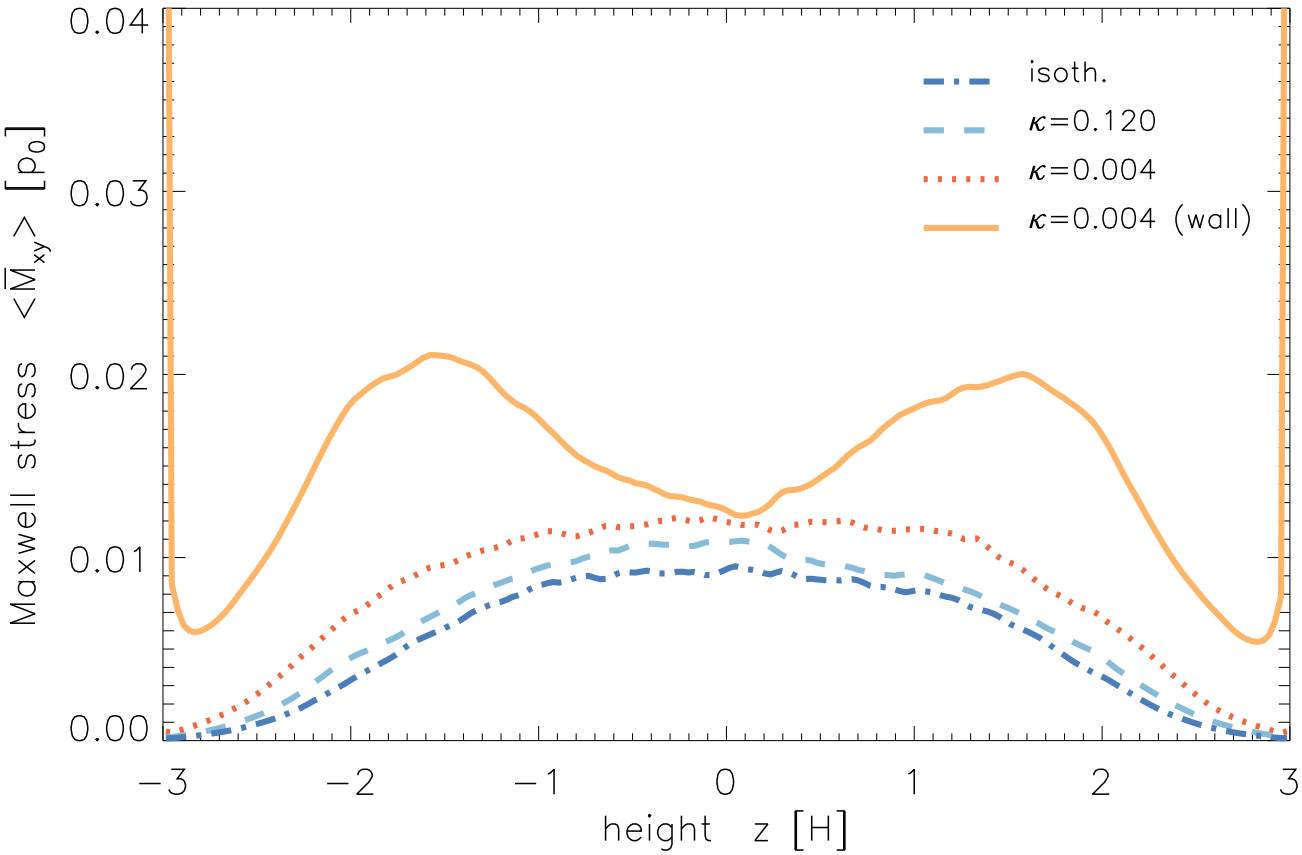

Maxwell stress density temperature heat flux

vertical disc structure

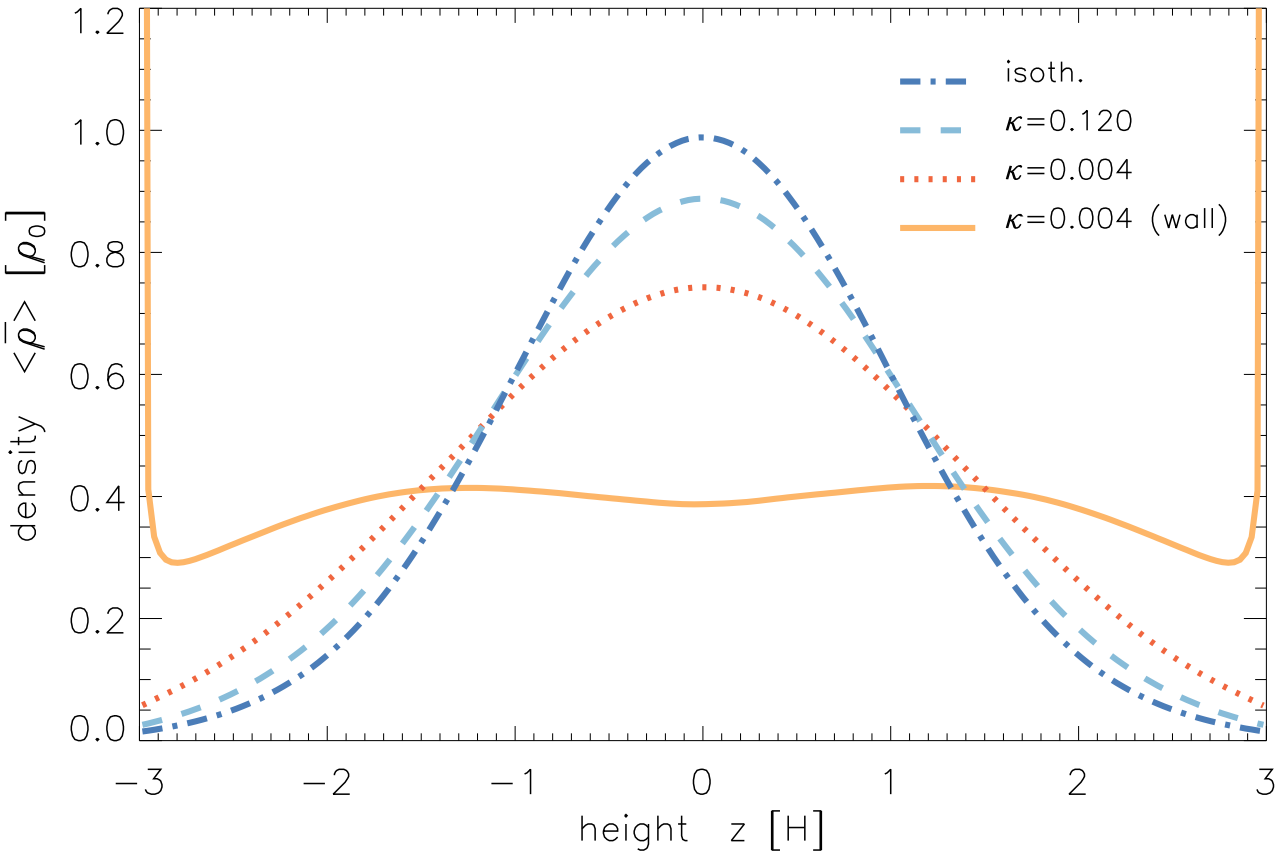

Maxwell stress **density** temperature heat flux

vertical disc structure

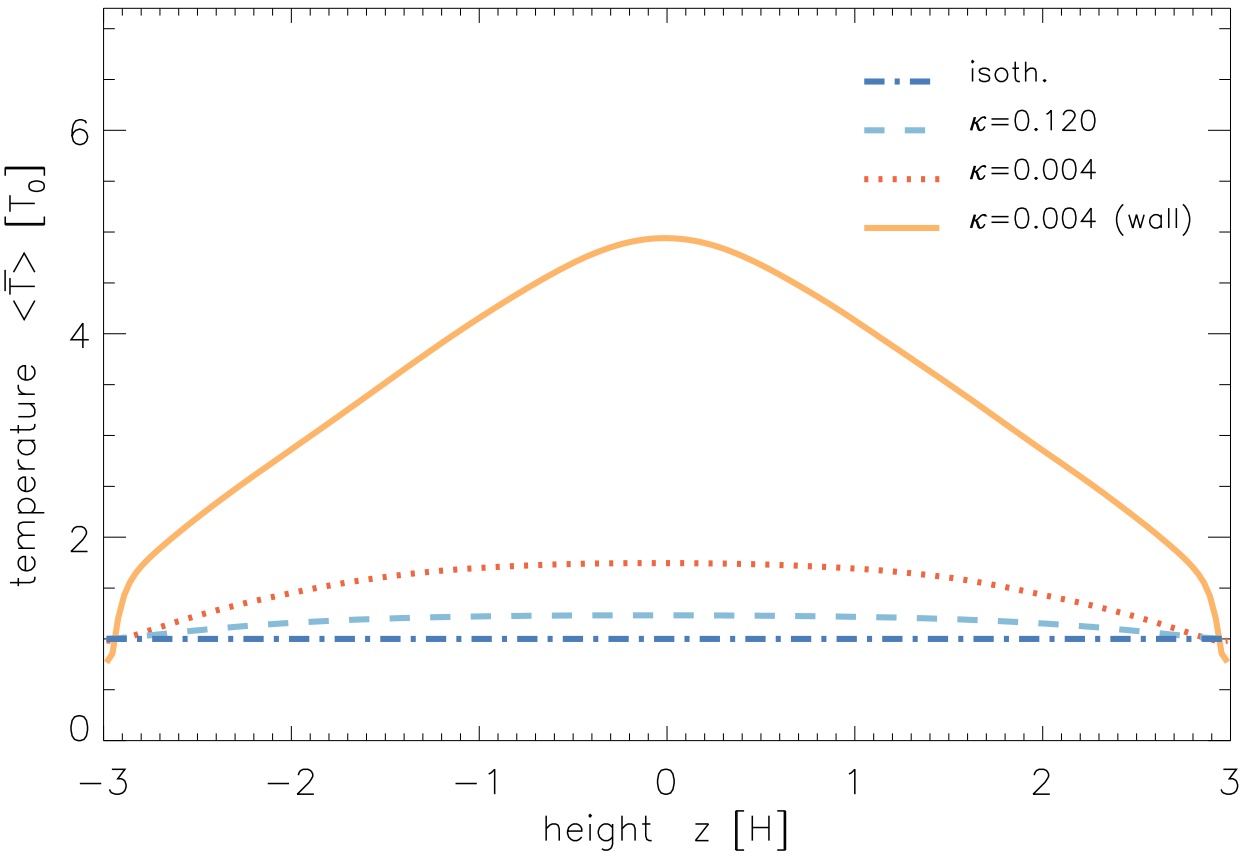

Maxwell stress density **temperature** heat flux

vertical disc structure

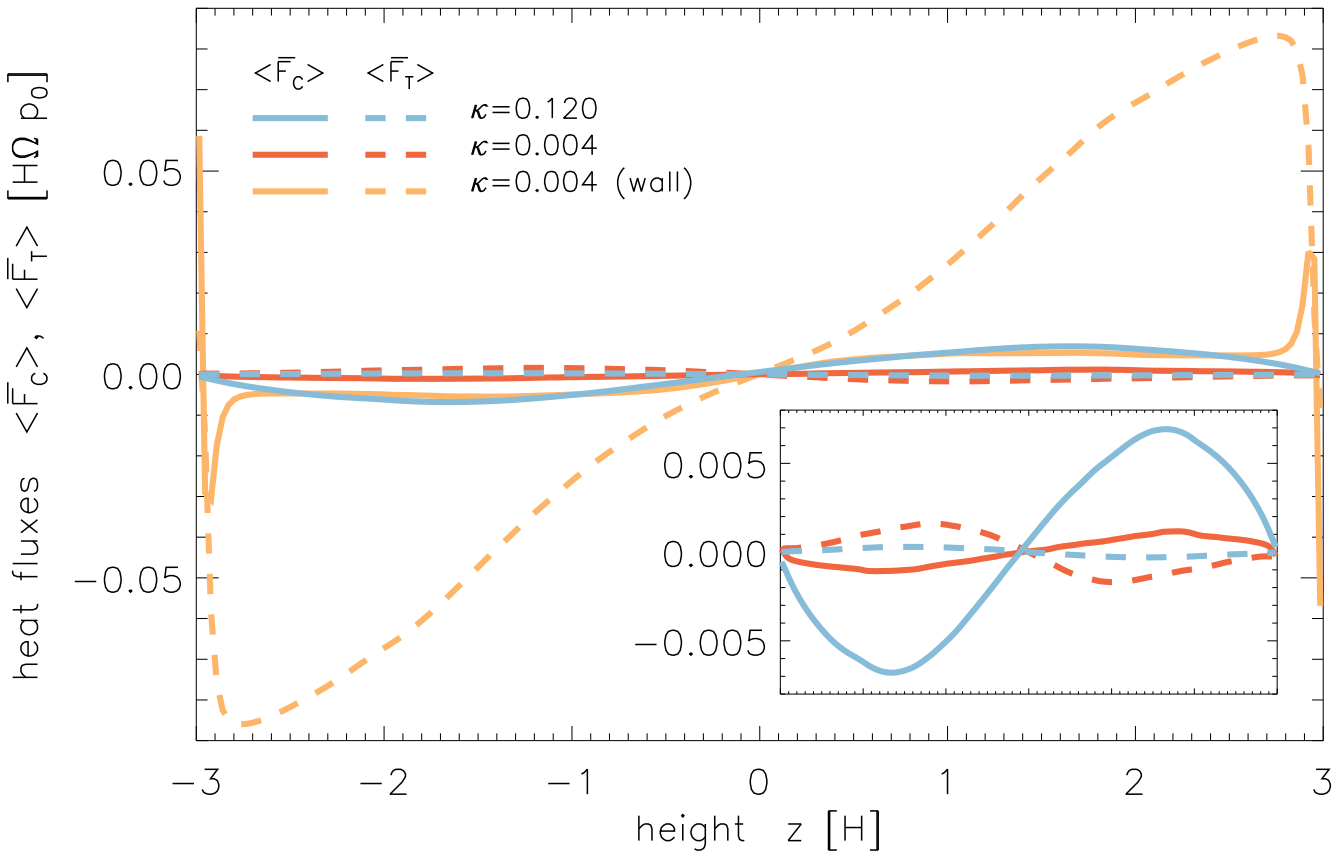

Maxwell stress density temperature **heat flux**

effect on mean-field dynamo

$\kappa = 0.120$ $\kappa = 0.004$ $\kappa = 0.004$ (wall)

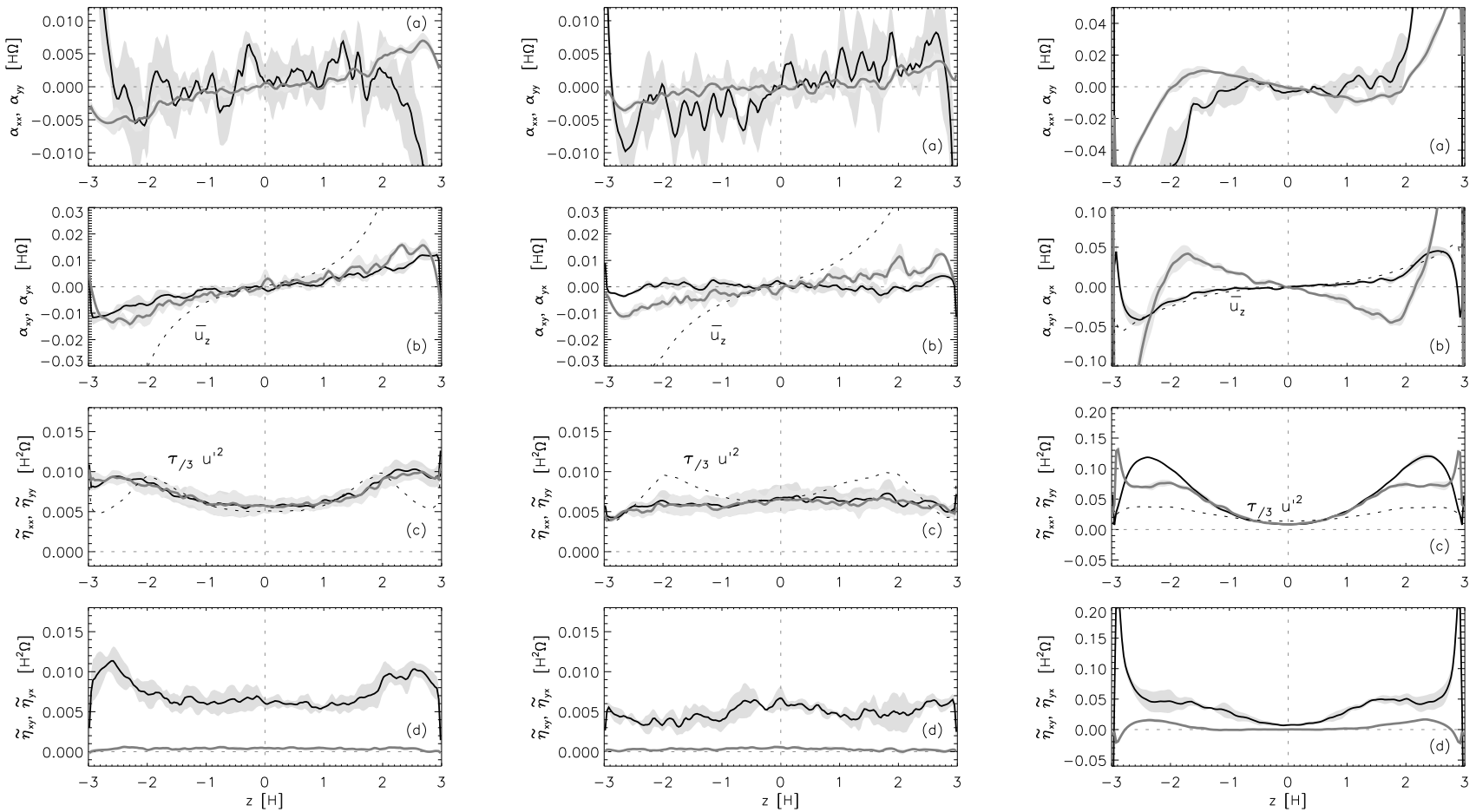

overview of results

Table 1
Summary of simulation results.

q	$\bar{B}_z^{\rm NVF}$	$T_{R\phi}^{\rm Reyn}$	$T_{R\phi}^{\rm Maxw}$	$T_{R\phi}^{\rm ratio}$	$P_{\rm cyc}$	$\tau_{\rm c}$	$u_{\rm rms}$	$\alpha_{yy}^{\rm peak}$	$\alpha_{yy}^{\rm buoy}$	$\eta_{yy}^{\rm peak}$	$\eta_{yy}^{\rm mid}$
	$[\beta_{\rm p\,800}]$	$[10^{-3}p_0]$	$[10^{-3}p_0]$		$[2\pi\Omega^{-1}]$	$[\Omega^{-1}]$	$[H\Omega]$	$[10^{-2}H\Omega]$	$[10^{-2}H\Omega]$	$[10^{-2}H^2\Omega]$	$[10^{-2}H^2\Omega]$
0.3	0.06	0.01 ± 0.00	0.24 ± 0.10	36.7	48.1	0.147	0.10 ± 0.03	0.106	−0.002	0.091	0.019
0.6	0.06	0.07 ± 0.03	1.13 ± 0.37	16.2	25.2	0.091	0.26 ± 0.08	0.386	−0.011	0.581	0.090
0.9	0.06	0.23 ± 0.09	2.12 ± 0.70	9.3	12.6	0.067	0.41 ± 0.12	0.673	−0.036	0.972	0.155
1.2	0.06	0.76 ± 0.26	4.47 ± 1.35	5.9	9.5	0.046	0.68 ± 0.15	0.936	−0.059	1.478	0.314
1.5	0.00	1.49 ± 0.46	5.88 ± 1.63	3.9	7.5	0.039	0.86 ± 0.14	1.048	−0.014	1.530	0.556
1.8	0.06	4.16 ± 1.02	11.75 ± 2.88	2.8	5.9	0.027	1.31 ± 0.06	1.200	–	1.513	1.232
1.5⋆	0.00	1.14 ± 0.37	4.99 ± 1.70	4.4	6.8	0.016	0.84 ± 0.01	0.867	−0.015	1.233	0.337
1.5	0.01	1.49 ± 0.44	5.88 ± 1.55	3.9	7.3	0.039	0.69 ± 0.03	1.031	−0.017	1.541	0.533
1.5	0.02	1.38 ± 0.39	5.48 ± 1.35	4.0	7.1	0.038	0.67 ± 0.03	1.107	−0.020	1.587	0.494
1.5	0.04	1.58 ± 0.55	6.26 ± 2.01	4.0	7.2	0.036	0.72 ± 0.02	1.023	−0.003	1.544	0.586
1.5	0.08	1.70 ± 0.53	6.75 ± 1.99	4.0	7.1	0.035	0.76 ± 0.02	1.100	−0.014	1.614	0.603
1.5	0.16	2.20 ± 0.57	8.81 ± 2.00	4.0	6.4	0.030	0.90 ± 0.03	1.149	–	1.833	0.703
1.5	0.32	3.57 ± 0.96	12.78 ± 2.73	3.6	5.9	0.018	1.20 ± 0.01	0.950	–	2.475	0.682
1.5	0.64	5.59 ± 3.00	15.06 ± 6.17	2.7	–	0.012	1.32 ± 0.03	0.655	–	4.425	0.436
1.5	1.28	5.32 ± 9.49	12.74 ± 11.33	2.4	–	0.019	1.11 ± 0.04	0.604	–	4.231	0.550

Notes: Here, the shear rate is defined as $q \equiv -{\rm d}\ln\Omega/{\rm d}\ln r$, that is, $q = 1.5$ for Keplerian rotation. The net-vertical field, $\bar{B}_z$, is given in units that are multiples of the field strength resulting in a midplane plasma parameter, $\beta_{\rm p}^{\rm mid} = 800$. The Reynolds and Maxwell stresses are computed as correlations of fluctuating quantities. The cycle period, $P_{\rm cyc}$, of the dynamo butterfly diagram is obtained as described in the text. The correlation time, $\tau_{\rm c}$, refers to the classic estimate of the turbulent diffusivity (cf. Fig. 5). In the chosen units, $u_{\rm rms}$ is equivalent of a turbulent Mach number. Dynamo coefficients labeled 'peak' ('buoy') correspond to open squares (triangles) in Fig. 3. The same holds for the turbulent diffusivity, which is plotted in Fig. 4, accordingly. The run marked with the asterisk (⋆) is a double-resolution reference run with $64/H$ grids, indicating that results are generally converged at the 20–40% level.

shear-rate dependence of stresses

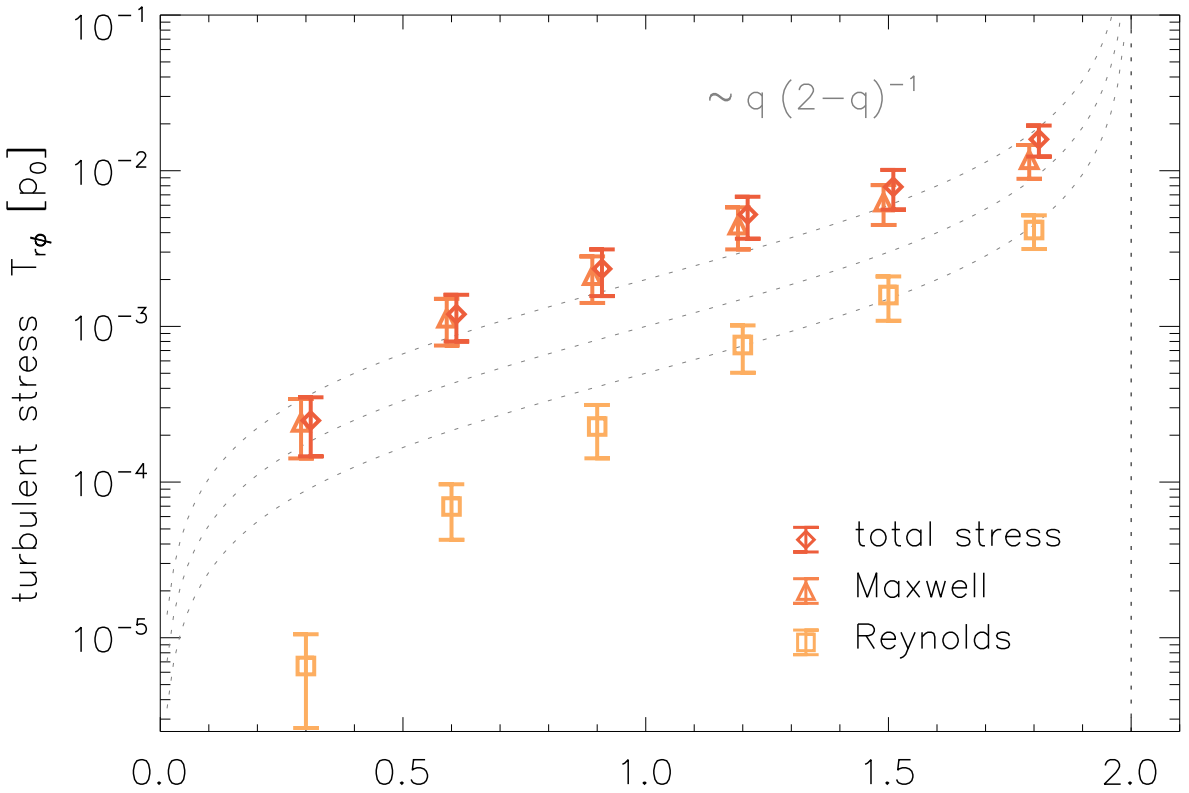

- Abramowicz, Brandenburg & Lasota (1996)
- Pessah, Chan & Psaltis (2006a/b,2008)
- Nauman & Blackman (2014)
- Gressel & Pessah (2015), ApJ 810, 59

shear-rate dependence of stresses

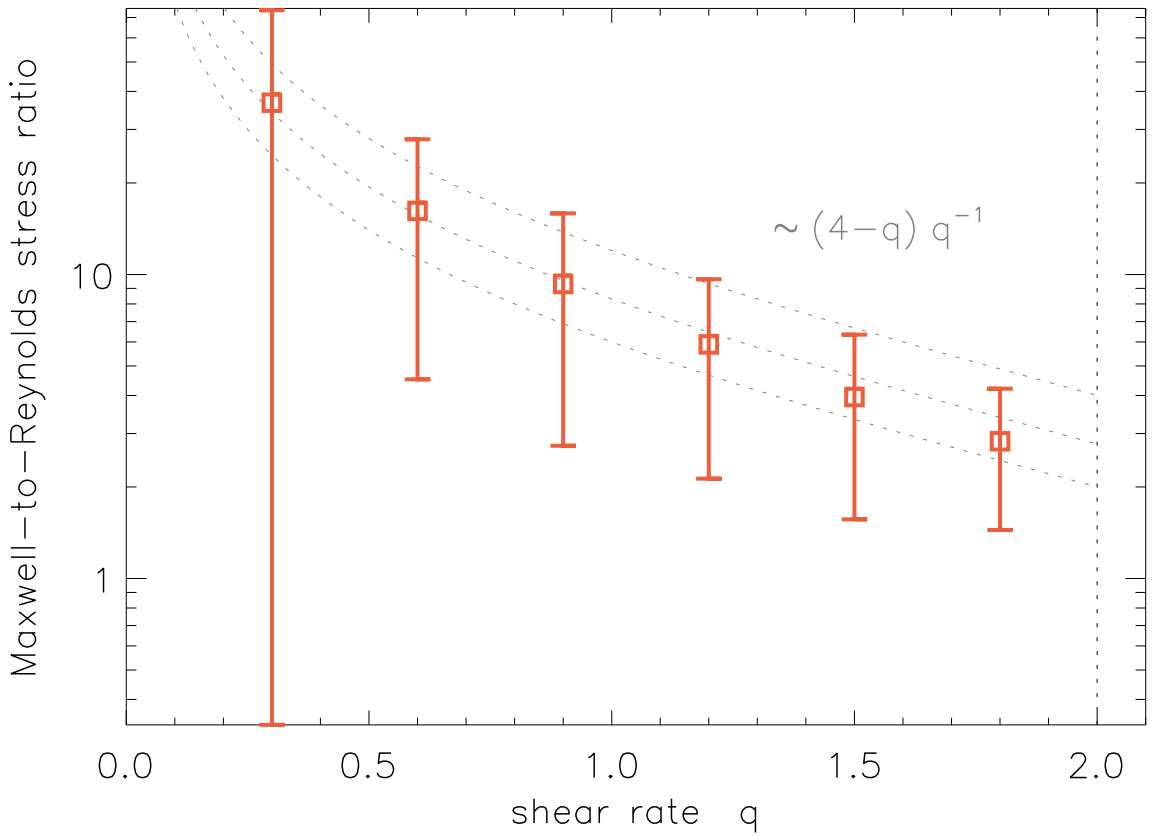

- Abramowicz, Brandenburg & Lasota (1996)
- Pessah, Chan & Psaltis (2006a/b,2008)
- Nauman & Blackman (2014)
- Gressel & Pessah (2015), ApJ 810, 59

net-vertical-field dependence of stresses

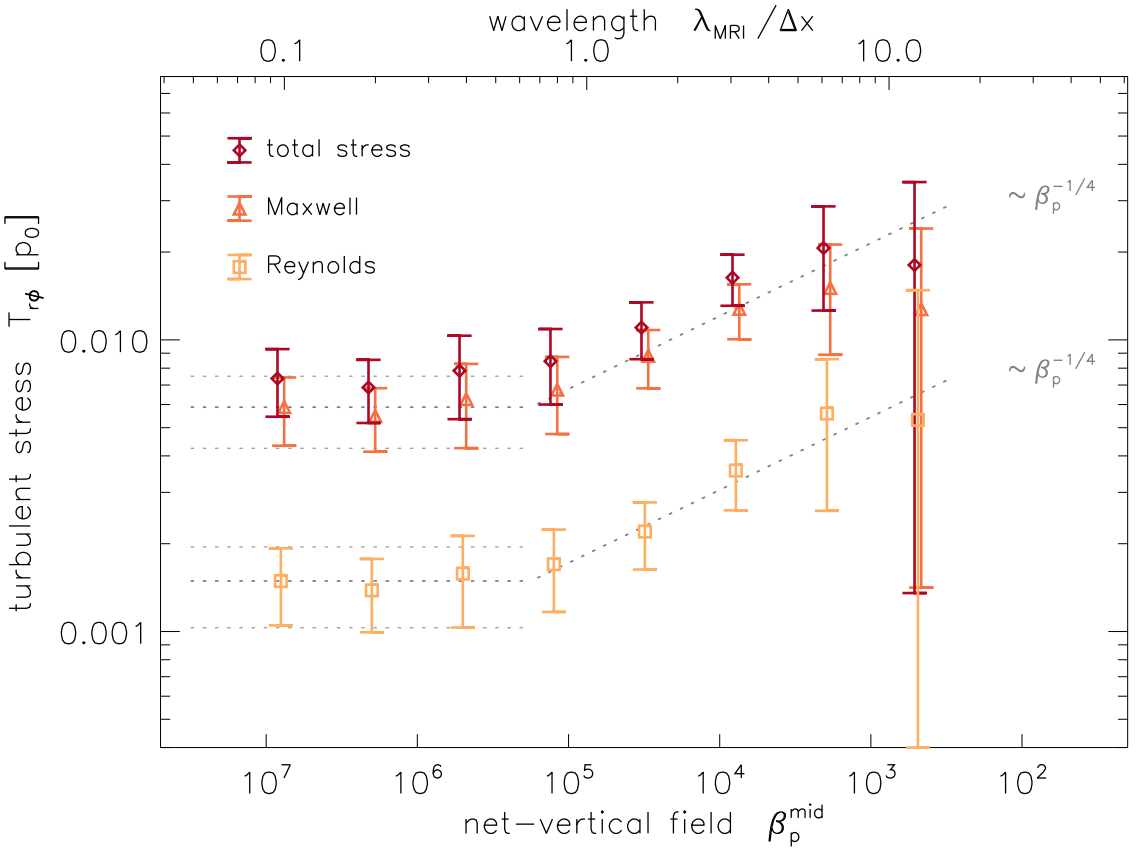

Sorathia+ (2010) Bai & Stone (2013a) Gressel & Pessah (2015) Salvesen+ (2016)

test-field α effect

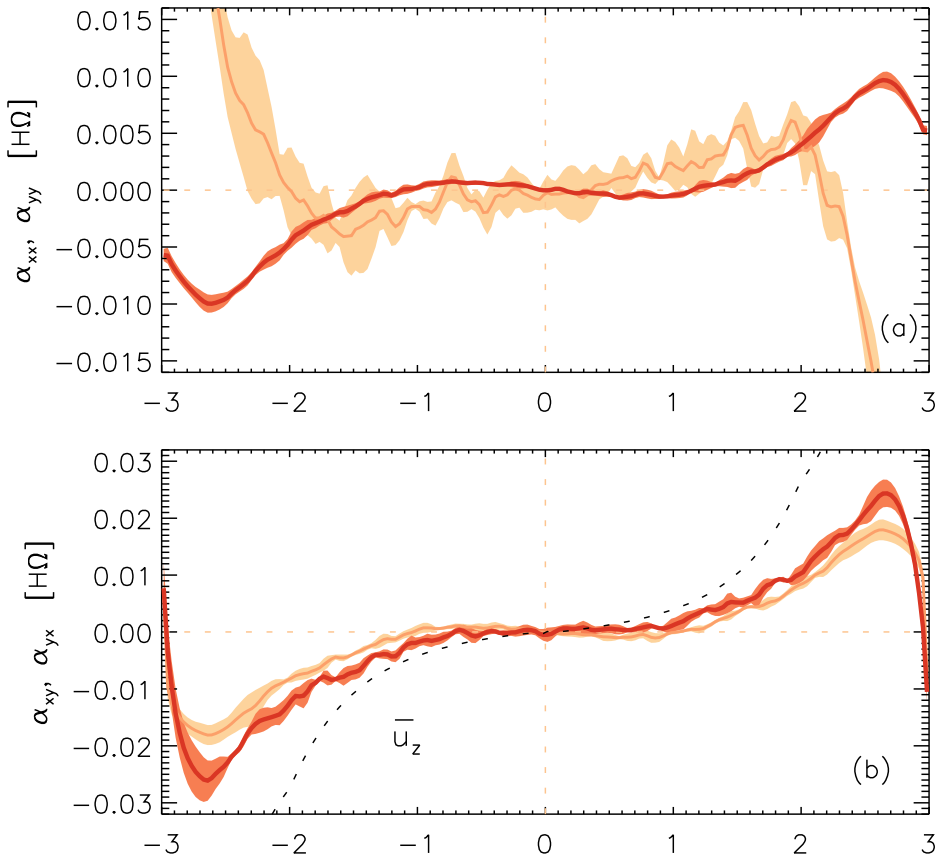

Gressel & Pessah (2015), ApJ 810, 59

- new test-field results for weaker shear of $q = 1.2$
- pronounced negative α effect near midplane
  Brandenburg (1998),
  Rüdiger & Pipin (2000)
- as previously: off-diagonal tensor elements both positive
  (dominant azimuthal fields)

test-field turbulent η

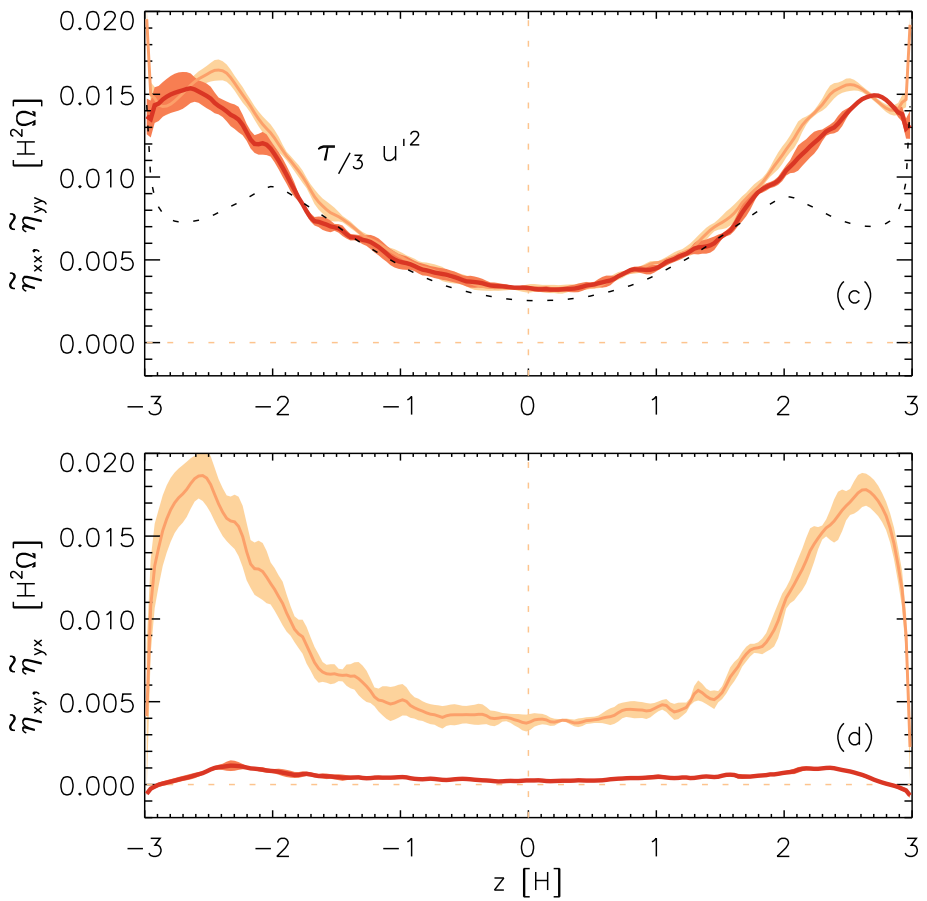

Gressel & Pessah (2015), ApJ 810, 59

- turbulent diffusion consistent with theory (for $z < 2\,H$)
- off-diagonals both positive
- weak $\tilde{\eta}_{yx}$ responsible for butterfly diagram?!

shear-rate dependence of dynamo coefficients

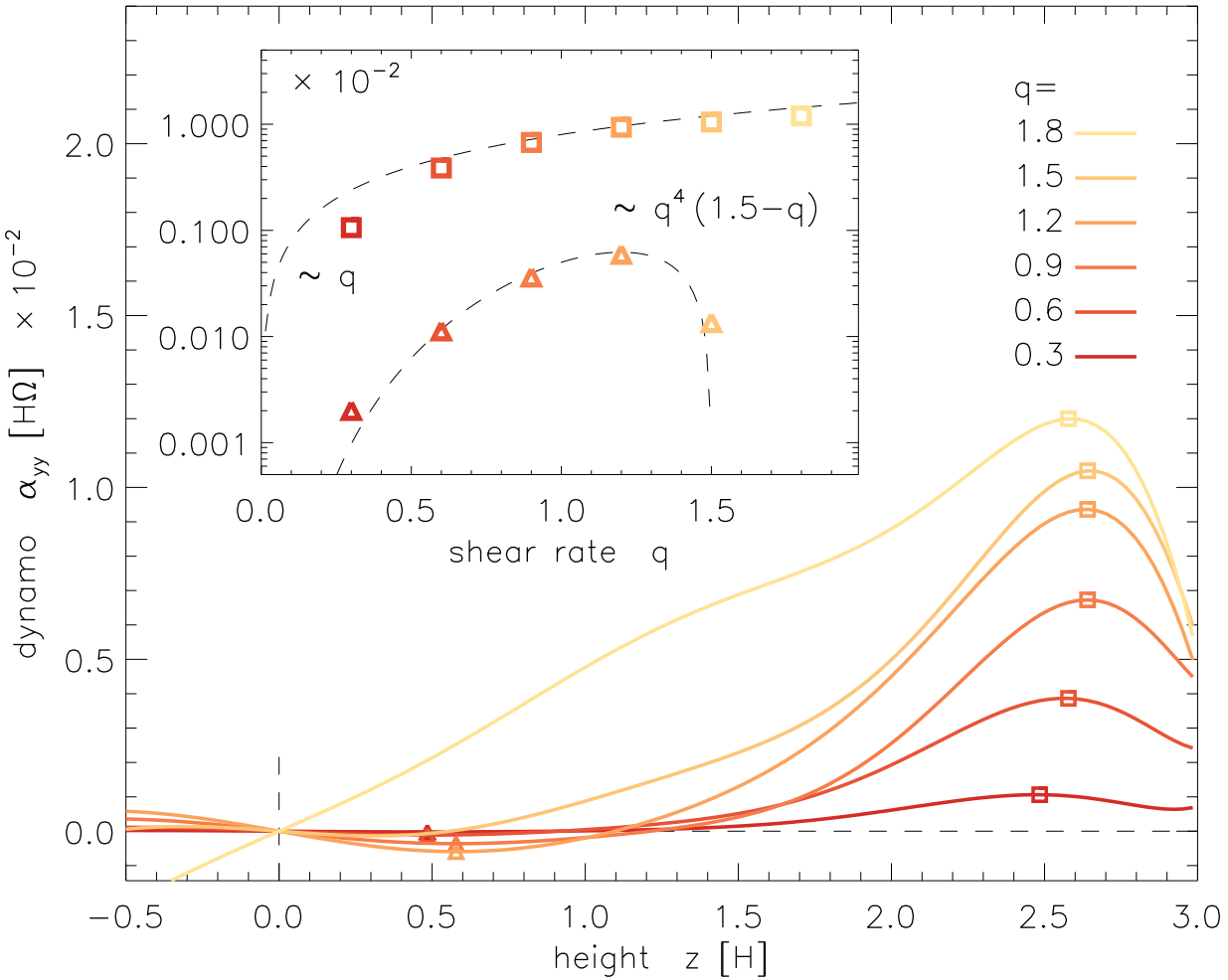

Rüdiger & Pipin (2000) Ziegler & Rüdiger (2001) Gressel & Pessah (2015), ApJ 810, 59

shear-rate dependence of dynamo coefficients

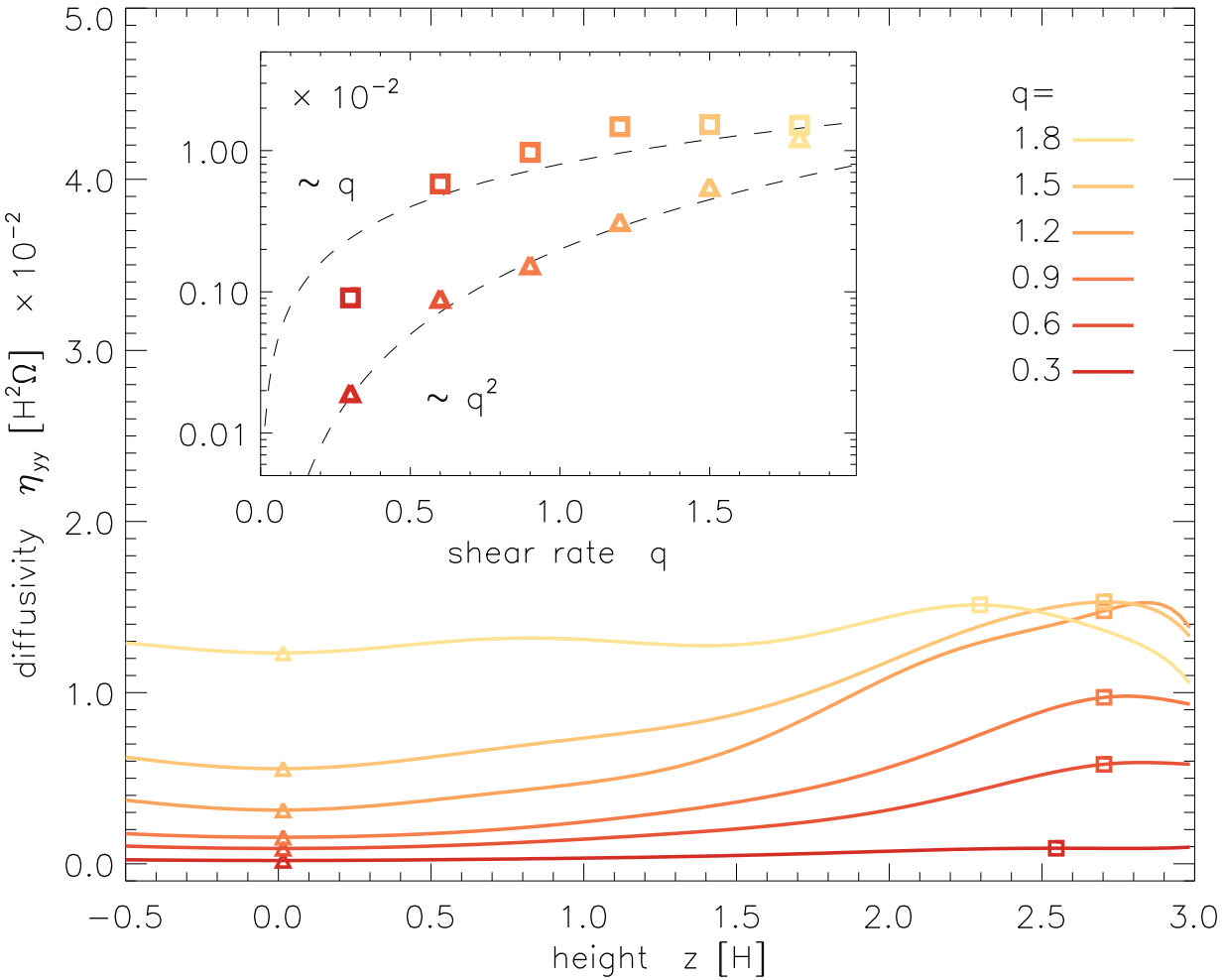

Rüdiger & Pipin (2000) Ziegler & Rüdiger (2001) Gressel & Pessah (2015), ApJ 810, 59

the dynamo cycle period

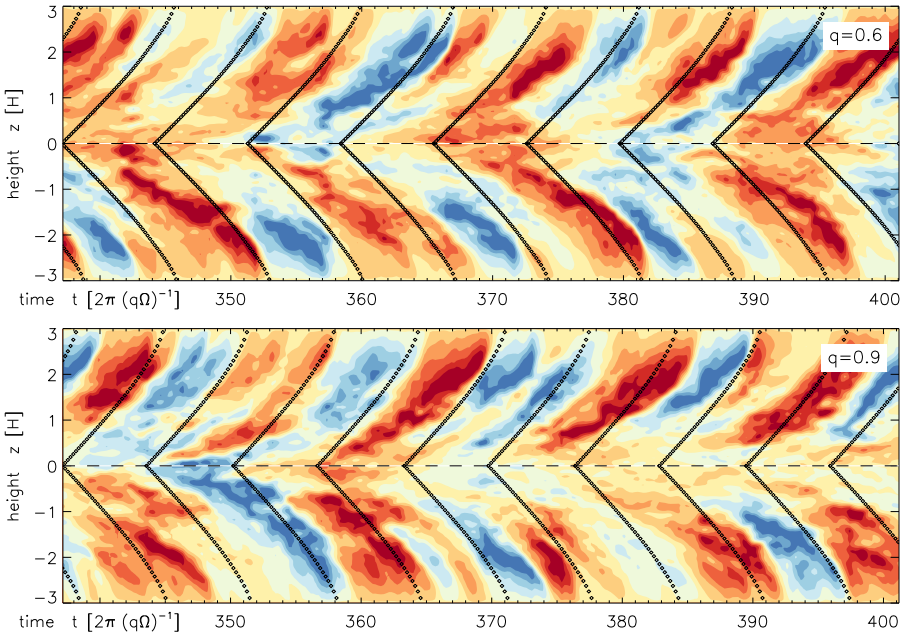

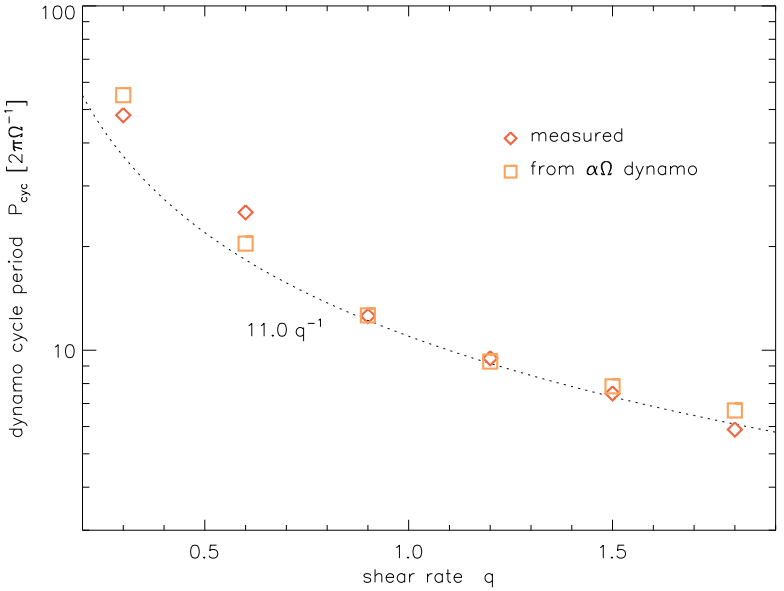

- $\omega_{\rm cyc} \simeq \left| \frac{1}{2}\, \alpha_{yy}\, q\Omega\, k_z \right|^{1/2}$
- shear-rate dependence explained by $\alpha\Omega$ dispersion relation
- fit-formula has $11\,\mathrm{yrs}$ as the constant
- propagation direction still “wrong”

Gressel & Pessah (2015), ApJ 810, 59

the dynamo cycle period

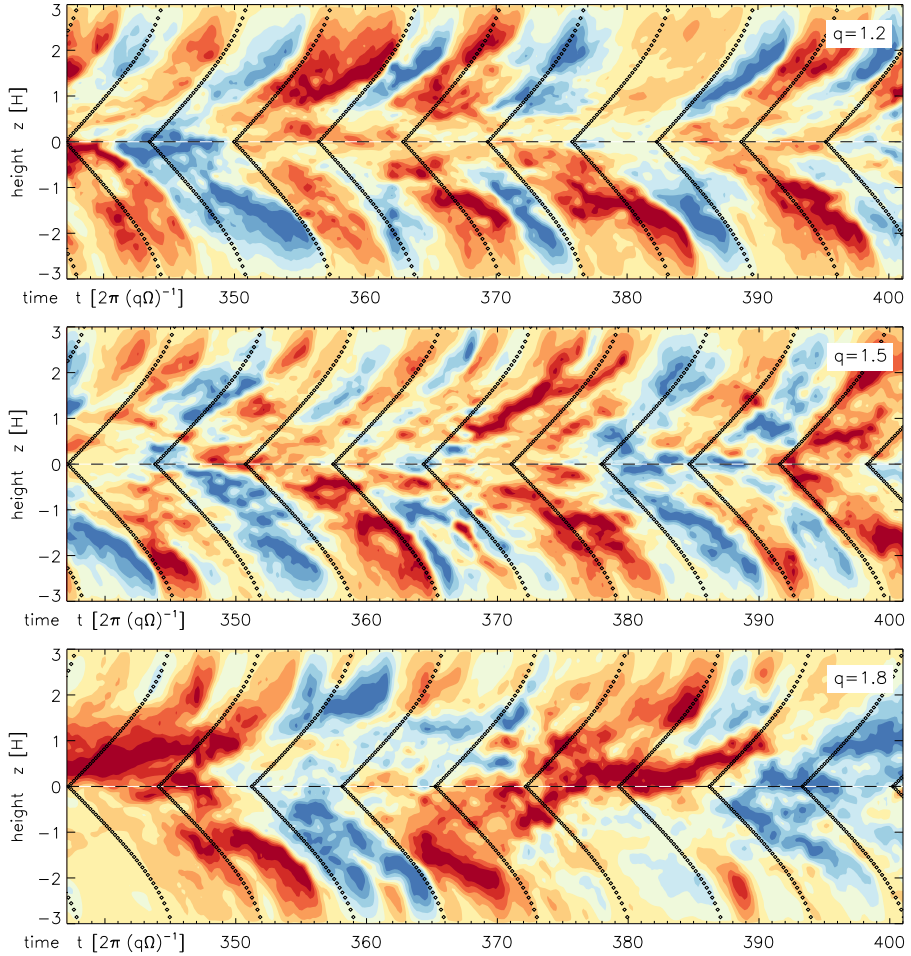

Gressel & Pessah (2015), ApJ 810, 59

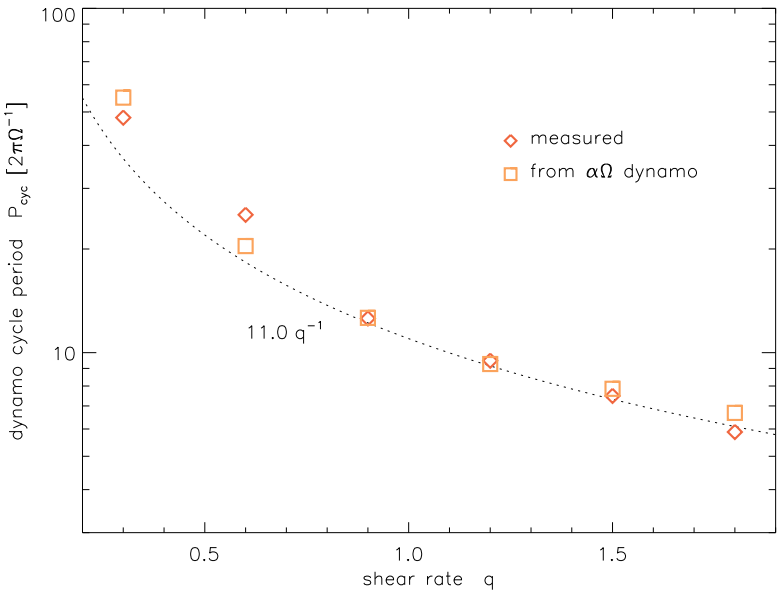

- $\omega_{\rm cyc} \simeq \left| \frac{1}{2}\, \alpha_{yy}\, q\Omega\, k_z \right|^{1/2}$
- shear-rate dependence explained by $\alpha\Omega$ dispersion relation
- fit-formula has $11\,\mathrm{yrs}$ as the constant
- propagation direction still “wrong”

net-vertical field dependence

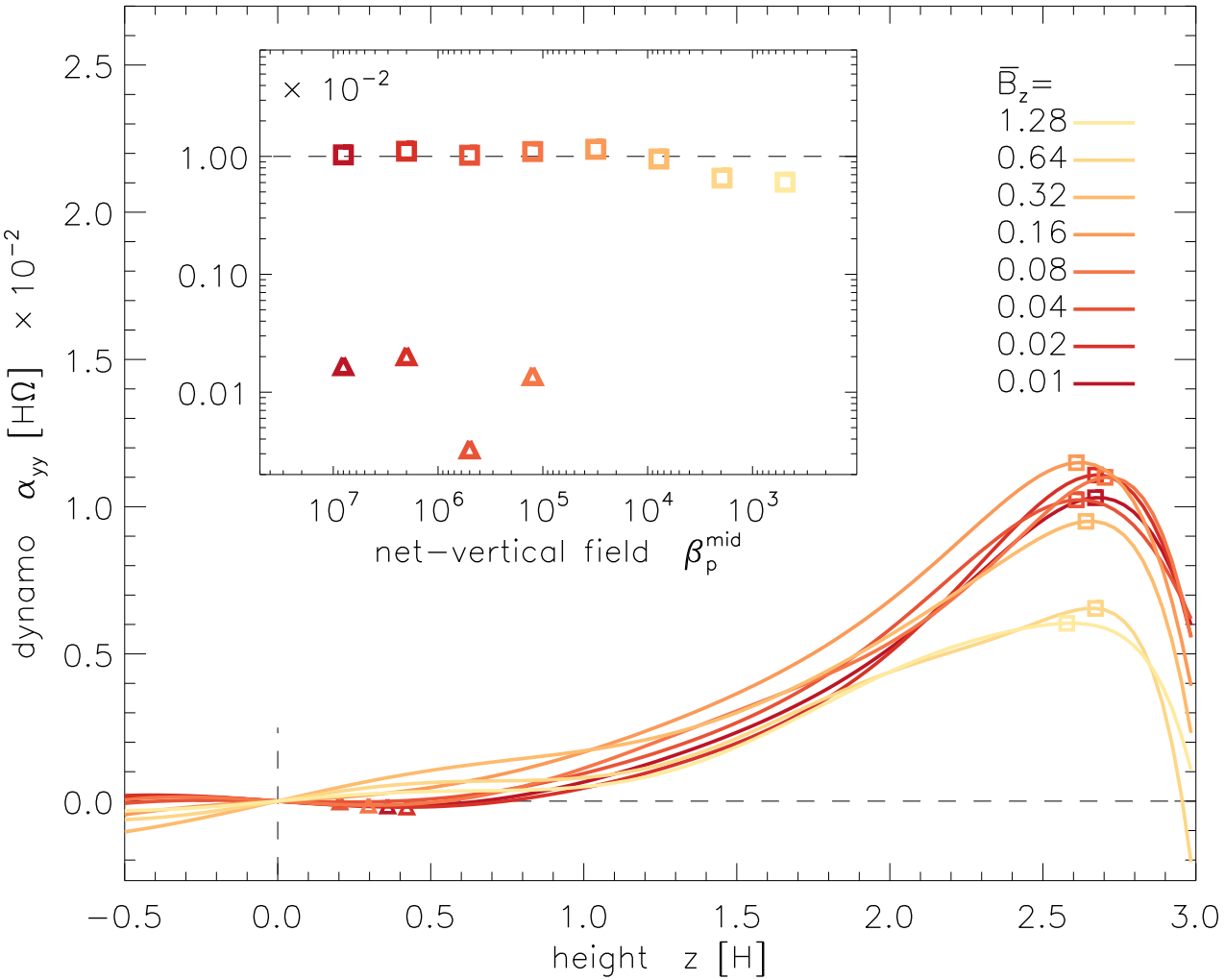

Gressel & Pessah (2015), ApJ 810, 59

net-vertical field dependence

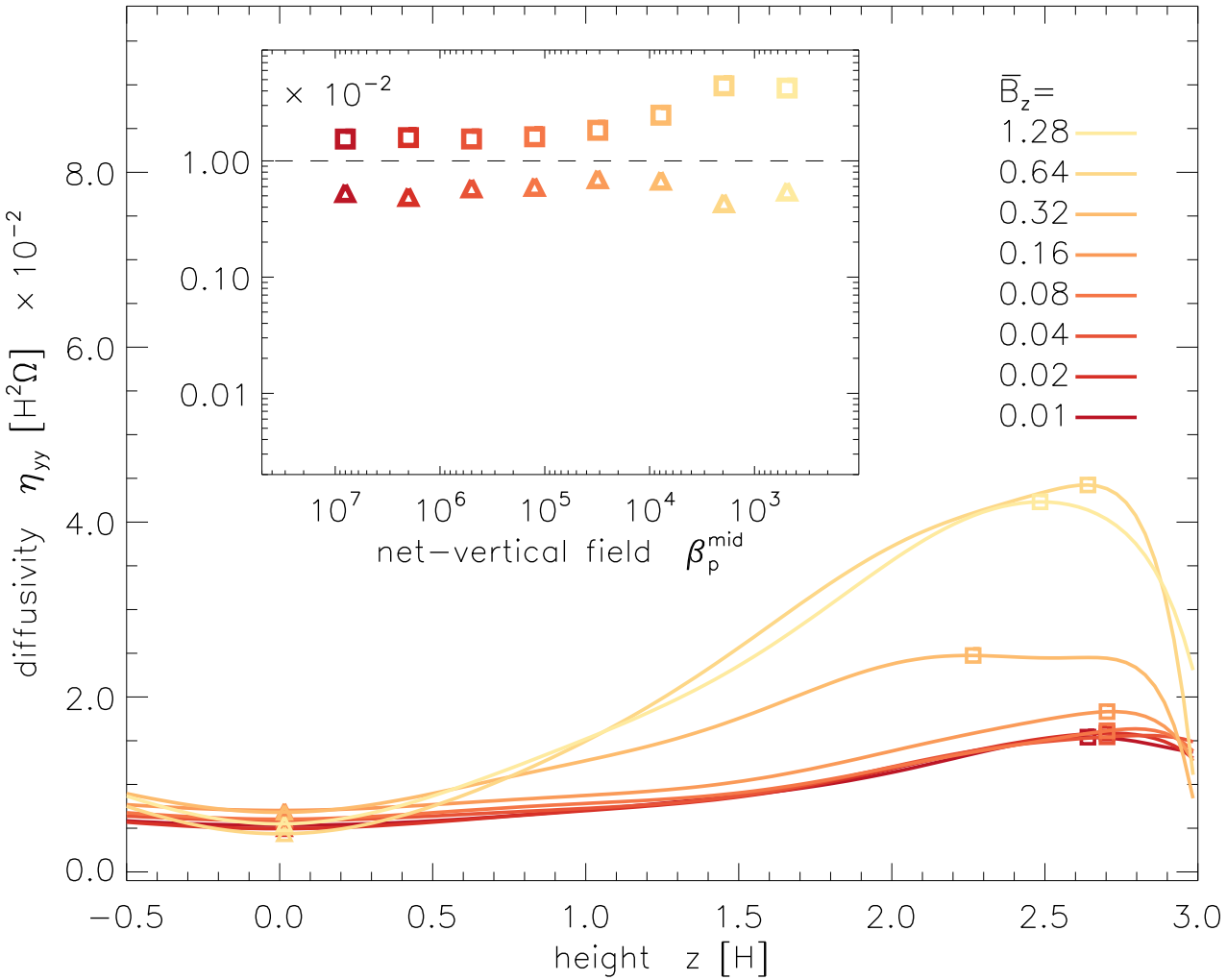

Gressel & Pessah (2015), ApJ 810, 59

non-local dynamo closure

- non-local formulation with $\hat{\alpha}$, $\hat{\eta}$ being convolution kernels

$$\bar{\mathcal{E}}_i(z) = \int \hat{\alpha}_{ij}(z,\zeta)\,\bar{B}_j(z-\zeta) \;-\; \hat{\eta}_{ij}(z,\zeta)\,\varepsilon_{jzl}\,\partial_z \bar{B}_l(z-\zeta)\,\mathrm{d}\zeta$$

- this translates to the Fourier amplitudes $\tilde{\alpha}(k_z)$, $\tilde{\eta}(k_z)$ being factors

$$\tilde{\bar{\mathcal{E}}}_i(k_z) = \tilde{\alpha}_{ij}(k_z)\,\tilde{\bar{B}}_j(k_z) \;-\; \tilde{\eta}_{ij}(k_z)\,\mathrm{i}k_z\,\varepsilon_{jzl}\,\tilde{\bar{B}}_l(k_z)$$

- convolution kernels can be characterized by Lorentzians,

$$\tilde{\alpha}(k_z) = \frac{\alpha_0}{1+(k_z/k_\mathrm{c})^2}\,, \qquad \tilde{\eta}(k_z) = \frac{\eta_0}{1+(k_z/k_\mathrm{c})^2}\,.$$

- convolution kernels in real space are decaying exponentials,

$$\alpha(\zeta) = \frac{\alpha_0}{2}\exp(-k_\mathrm{c}^{(\alpha)}\,|\zeta|\,)\,, \qquad \eta(\zeta) = \frac{\eta_0}{2}\exp(-k_\mathrm{c}^{(\eta)}\,|\zeta|\,)\,,$$

scale-dependence of dynamo coefficients

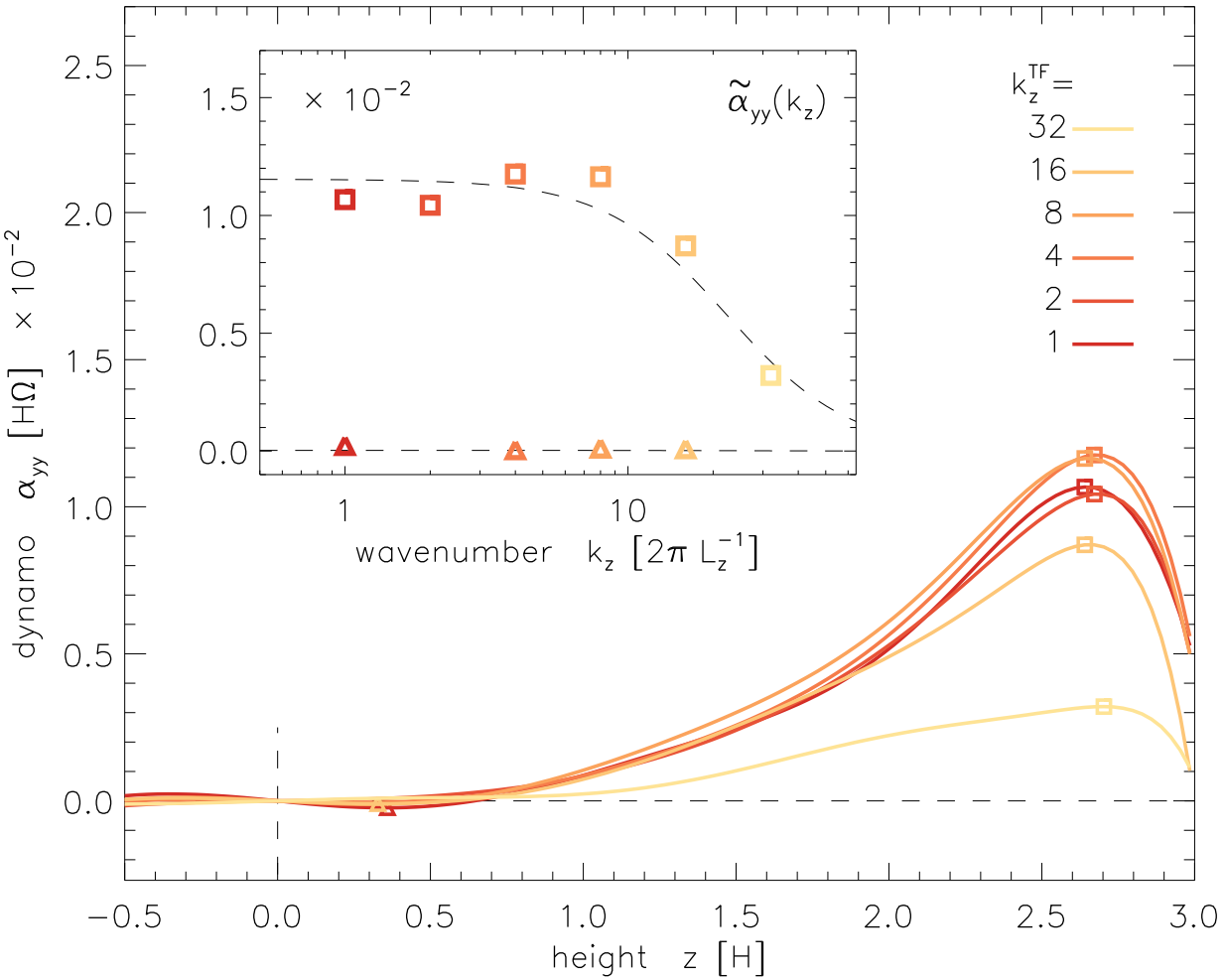

Gressel & Pessah (2015), ApJ 810, 59

scale-dependence of dynamo coefficients

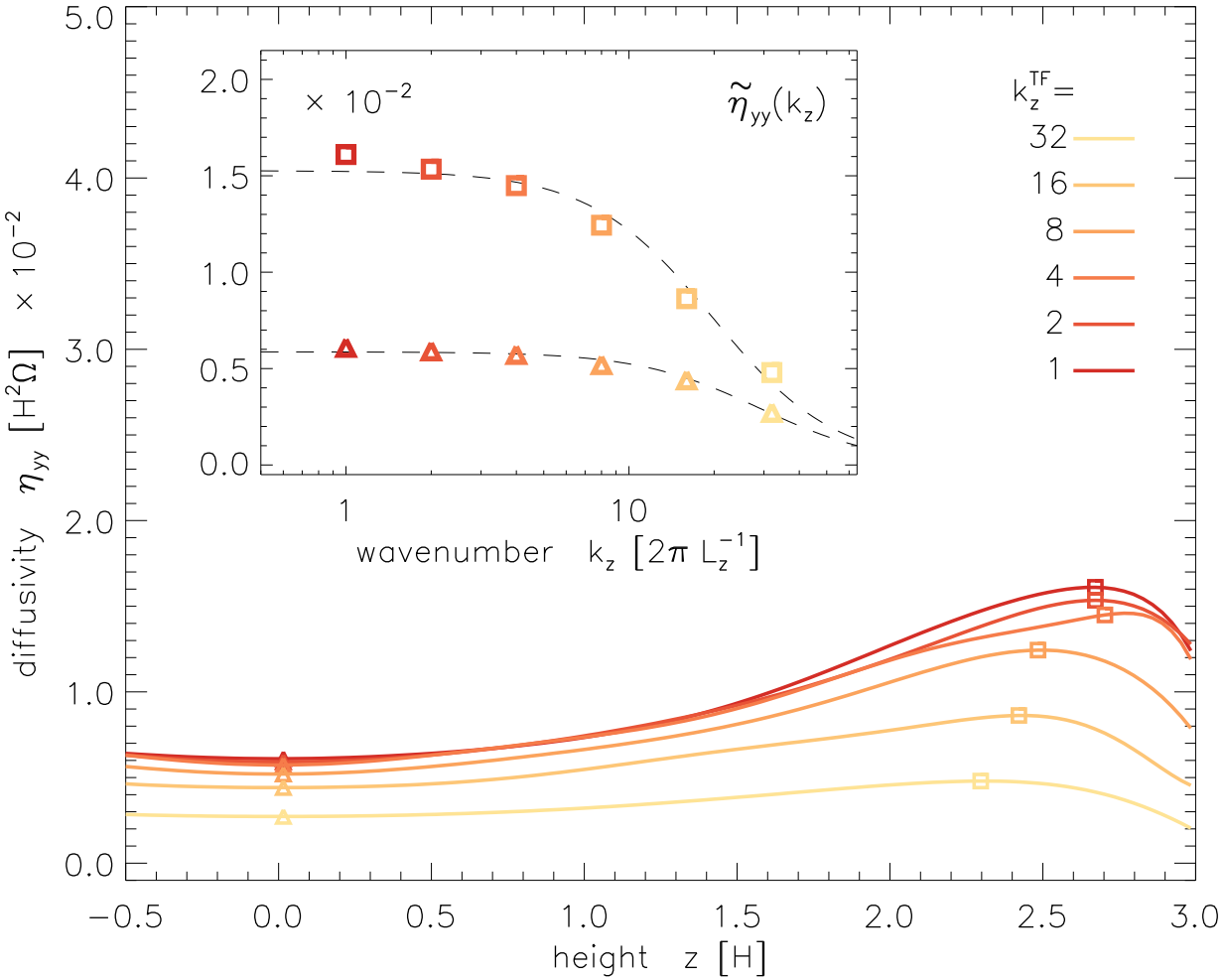

Gressel & Pessah (2015), ApJ 810, 59

summary of results

- I. Mean-field Dynamo in stratified MRI
  - test-field diagnostics are a useful tool
  - butterfly can be reproduced by a simple toy model
  - precise origin of dynamo effect still unidentified
- II. Effect of the convective state of the disc
  - inefficient thermal conduction leads to a convective state
  - overturning motions drastically affect the dynamo
  - may explain classical S-curve disc instability models
- III. Shear-rate dependence of the dynamo
  - dynamo cycle period well explained as function of shear-rate
  - promising non-local formulation (may explain “wrong” propagation)
  - established the scale-separation ratio of the MRI dynamo

summary of results

- I. Mean-field Dynamo in stratified MRI
  - test-field diagnostics are a useful tool
  - butterfly can be reproduced by a simple toy model
  - precise origin of dynamo effect still unidentified
- II. Effect of the convective state of the disc
  - inefficient thermal conduction leads to a convective state
  - overturning motions drastically affect the dynamo
  - may explain classical S-curve disc instability models
- III. Shear-rate dependence of the dynamo
  - dynamo cycle period well explained as function of shear-rate
  - promising non-local formulation (may explain “wrong” propagation)
  - established the scale-separation ratio of the MRI dynamo

summary of results

- I. Mean-field Dynamo in stratified MRI
  - test-field diagnostics are a useful tool
  - butterfly can be reproduced by a simple toy model
  - precise origin of dynamo effect still unidentified
- II. Effect of the convective state of the disc
  - inefficient thermal conduction leads to a convective state
  - overturning motions drastically affect the dynamo
  - may explain classical S-curve disc instability models
- III. Shear-rate dependence of the dynamo
  - dynamo cycle period well explained as function of shear-rate
  - promising non-local formulation (may explain “wrong” propagation)
  - established the scale-separation ratio of the MRI dynamo